PHILOSOPHICAL TRANSACTIONS OF THE ROYAL SOCIETY A MATHEMATICAL, PHYSICAL & ENGINEERING SCIENCES

The Seismicity, Geomorphology and Structural Evolution of the Corinth Area of Greece

C. Vita-Finzi and G. C. P. King

Phil. Trans. R. Soc. Lond. A 1985 **314**, 379-407
doi: 10.1098/rsta.1985.0024

Phil. Trans. R. Soc. Lond. A **314**, 379–407 (1985) [379]
Printed in Great Britain

THE SEISMICITY, GEOMORPHOLOGY AND STRUCTURAL EVOLUTION OF THE CORINTH AREA OF GREECE

By C. VITA-FINZI† and G. C. P. KING‡

† *Department of Geography, University College London, Gower Street, London WC1 6BT, U.K.*
‡ *Bullard Laboratories, Department of Earth Sciences, Madingley Rise, Cambridge CB3 0EZ, U.K.*

(*Communicated by D. H. Matthews, F.R.S. – Received 9 May* 1984)

[Plates 1 and 2]

CONTENTS

In the eastern Gulf of Corinth, geological structure is closely reflected in the topography. In the 1981 Corinth earthquakes ground deformation accentuated existing geomorphological patterns. We explore the relationship between seismicity and landforms in space and time. The area examined extends beyond the epicentral region of the 1981 events and its evolution is traced over the last 40000 years.

To understand the relation between deep and superficial structures we discuss processes that occurred in the 1981 earthquakes, and go on to propose that surface faulting appears only above linear faults at depth that move in earthquakes with magnitudes (M_s) greater than six. Where faults at depth intersect or bend, the faulting becomes distributed and primary faulting does not reach the surface. Here the surface manifestation of faulting at depth is surface folding and secondary faulting. Such regions are identified in maps of the eastern Gulf of Corinth.

Evidence for the evolution of the fault systems is provided by eyewitness accounts

of shoreline changes following the recent earthquakes, historical and archaeological data pertaining to old sea levels, and ^{14}C dates for molluscs collected from fossil shorelines.

The results of these studies broadly confirm an earlier view of J. A. Jackson *et al.* (*Earth planet. Sci. Lett.* **57**, 377–397 (1982)) that motion has shifted from faulting south of the city of Corinth to faulting in the Perachora peninsula. But the transfer is not complete: areas lying between the two fault systems have moved up and down in historical and archaeological times indicating that both systems are still active. The evidence for activity of the northern system points to a repeat time of 300 years for earthquakes comparable with those of 1981.

The work discussed in this paper suggests that some of the features previously described as marine terraces are fault-controlled continental surfaces. Furthermore, beach deposits at a number of different levels long regarded as successive shorelines are in fact contemporaneous. The critical ages were obtained by radiocarbon dating of shell carbonate, a technique which yields dependable results if applied to samples which have been carefully selected and pretreated. Palaeontological dating of the terraces, in contrast, is found to be misleading because the faunas are environmentally controlled and consequently diachronous.

1. Introduction

The purpose of this paper is to show how the recent structural evolution of a normal fault system may be investigated by using a combination of field mapping, geomorphological interpretation, archaeological and radiometric dating and the results of the analysis of seismic records. The fieldwork on which the paper draws called for a reassessment of the evidence on which the late Quaternary marine chronology of the Mediterranean rests. It also included a study of the structures associated with 'barrier' zones of fault systems, that is the zones where earthquake rupture starts and stops. An ability to interpret correctly the surface manifestation of 'barrier' faulting at depth is vital to progress in understanding the physics of earthquakes and to the development of systematic methods of earthquake prediction.

The region we chose to examine is the eastern end of the Gulf of Corinth in Greece (figure 1). It was selected for two reasons. First, it was struck in 1981 by three earthquakes which produced extensive surface faulting (Jackson *et al.* 1982) and for which an aftershock study was available (King *et al.* 1984). Second, archaeological sites and raised beaches in the area suggested that we might be able to trace vertical motions back beyond the period spanned by eyewitness accounts. A problem is that parts of the region are composed of limestone lacking distinctive internal horizons, so that in some places faults and folds have to be inferred from landforms. Doing this is not entirely straightforward as the pre-faulting landscape was far from flat. An inspection of the unfaulted zones north and south of the Gulf, however, allowed the distinctive features of the faulted and folded landscape in the field area to be recognized and mapped.

The framework for this study is the model for the evolution of the region proposed by Jackson *et al.* (1982). Their scheme is shown in the insert to figure 1 and may be summarized as follows. In late Tertiary times motion occurred on faults south of the city of Corinth. One consequence was that the hanging wall of these faults subsided and became covered with marine sediments. Movement later shifted to faults north of the city (the faults that moved in the recent earthquake) and produced many of the features that are now visible. The upper surface of the hanging-wall block of the northern faults now lies beneath the deep eastern part of the Gulf

PHILOSOPHICAL TRANSACTIONS OF THE ROYAL SOCIETY A MATHEMATICAL, PHYSICAL & ENGINEERING SCIENCES

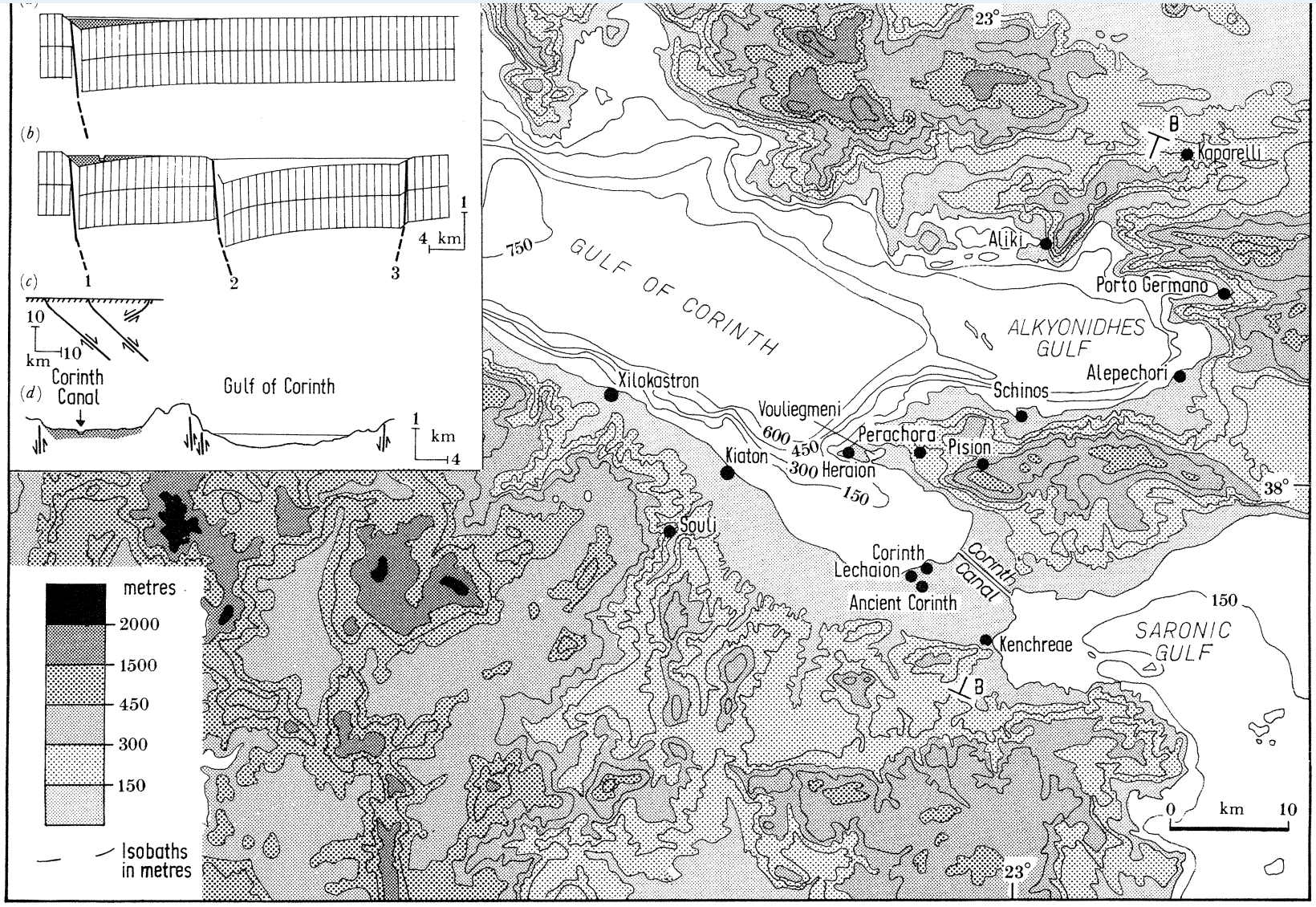

FIGURE 1. Location map showing topography and place names referred to in text. The inset summarizes important features of the model described in Jackson *et al.* (1982) and based on the techniques of Mansinha & Smylie (1971), and the evolution of a section corresponding to BB′ on this map and figure 2. In (*a*) the deformation associated with motion on the southern fault system alone is shown. The shading indicates marine sediment. In (*b*) the faults on the northern margin of the Perachora peninsula have moved to form the eastern Gulf of Corinth. The process causes uplift of the sediment deposited in the first phase of movement. The geometry of faulting used in the model is shown in (*c*) and a cross section of the present topography is shown in (*d*).

of Corinth (the Alkyonidhes Gulf), whereas areas that had previously subsided have been uplifted to expose marine sediments such as those that form the Corinth isthmus and those associated with various elevated shorelines.

The model of Jackson *et al.* (1982) was based on an examination of surface faulting and on preliminary seismic information. In this paper, which is based on fieldwork carried out in July and August 1982, we extend the study over a larger area and further back in time. We start, in §2, with a review of earlier discussions of the 1981 surface breaks and the related seismic evidence. Some of the field descriptions are amended to take account of new observations; relevant information from the aftershock study of King *et al.* (1984) is incorporated; and the nature of the structures associated with the Perachora peninsula is discussed. The peninsula is identified as a 'barrier' in the sense proposed by Aki (1979) and extended by King & Yielding (1984) and King (1984). The multiple faulting at depth that is suggested by the aftershock pattern apparently produces features which differ from those of the main fault scarps.

The form of these structures is discussed and some ideas required to understand the relation between fault motion at depth and directly observable surface features are introduced. These are illustrated by a series of schematic models. A key point of the discussion is that in regions of multiple faulting at depth the only manifestations of subsurface faulting may be superficial folding and secondary faulting. Primary faults need never reach the surface. The concepts are used to produce structural maps for the eastern Gulf. It may seem unorthodox to present models before a discussion of the surface features that we seek to explain, but we think that the examples are more readily understood if the reader already has the final models in mind.

The structural maps of the eastern Gulf of Corinth show that the fault pattern is too complex to be accommodated in the original model. An improved scheme is used in §4 as the basis for discussing a plausible structural history for the region.

In §3 we discuss features which may be used to establish a chronology for the evolution of the fault system. Historical and archaeological sites which reflect changes of land level relative to sea level are examined first. Next we discuss raised beach and elevated marine deposits whose age is established by ^{14}C dating of shell material. Palaeontological dating is considered and is found to be unhelpful for the late Quaternary because many of the mollusc assemblages that have been employed to develop chronologies of Mediterranean stratigraphy are diachronous and their distribution depends mainly on environment (see Richards 1982).

Finally, in §4, the dated changes of land level and the fault model for the region (from §2) are combined to describe the evolution of faulting in the eastern Gulf of Corinth. A repeat time of 300 years for earthquakes of the type that occurred in 1981 is suggested.

2. Structures in the eastern Gulf of Corinth

The Gulf of Corinth has long been considered to be a rift valley or graben structure. It is roughly 150 km long and 20 km wide. The northern shore is bordered mainly by Mesozoic limestones, whereas the southern consists largely of Neogene clastic deposits. The water depth is about 1000 m and the height of the surrounding prefaulted Tertiary topography is also about 1000 m. Thus 2000 m of relative vertical motion has taken place but, bearing in mind the presence of sea-floor sediment up to 1 km thick (Brooks & Ferentinos 1984), this must be regarded as a minimum figure.

Rift valleys are often assumed to be symmetrical structures but it is now apparent from a

number of well studied regions that they are not (McKenzie 1978; Bally 1982). The Gulf of Corinth appears to be no exception (Heezen *et al.* 1966). Asymmetry is evident from maps of the region. The northern side of the Gulf has a drowned coastline, whereas the southern side is emergent. This arises because the faulting that dips to the north is apparently more important than the antithetic faulting to the north. The seismic information and the more detailed consideration of the morphology that we now discuss for the eastern end of the Gulf add further substance to this view.

(*a*) *Deformation in the 1981 earthquakes*

The three earthquakes that occurred on 24 and 25 February and 4 March 1981 were associated with clear surface deformation (Mariolakos *et al.* 1982). The surface ruptures, fault plane solutions and relocations for the main events were discussed by Jackson *et al.* (1982). This information is summarized in figure 2 together with data from a preliminary aftershock study (King *et al.* 1984). It was noted in these papers that in many places the major faults controlled the morphology and that some of the faults had moved in the earthquake. Where the faults crossed the coast some regions had risen relative to sea level whereas others had dropped (figure 3).

For practical reasons these changes could not be determined with any accuracy in the period immediately following the earthquake. After more than a year of observation, seaside taverna owners and fishermen who operate small boats around the coast could resolve sea-level changes to better than 10 cm for subsidence and somewhat worse for uplift. The asymmetry can be explained as follows. Where the land had sunk, tracts of coast that were always above high water before the earthquake were covered by high tide afterwards. Features such as mooring rings in regular use provided accurate reference levels. Where uplift had occurred, its extent had to be gauged from the position of unfamiliar features exposed at low tide, and the results are consequently less reliable.

It became clear in the course of these enquiries that many myths were generated soon after the earthquake, and people described with confidence effects which were later found to be fictitious. In the village of Schinos, for instance, we were informed that sea level had continued to change for some weeks after the earthquake. Fishermen who constantly used landing points in the harbour, however, were adamant that no such change had been perceptible and indicated the exact points of the post-earthquake high water on which they based their statements. At Skaloma, the wife of a fisherman declared that there had been no change of sea level but her husband showed us in several places exactly where high water level reached before and after the earthquake. Great care was therefore taken to ensure that our informants were reliable. The points where sea level changes were determined are shown in figure 3.

In Jackson *et al.* (1982) it was implied that the Perachora peninsula had probably risen after the earthquake as a result of motion on a NE–SW striking portion of the undersea fault that was thought to have moved in the first event (figure 2, CC′). Since it turns out that the peninsula sank, this segment evidently did not move appreciably in the 1981 event.

With the foregoing modification included, figure 2*c* shows a simplified diagram of the faulting responsible for the 1981 events. The first earthquake was initiated near the Perachora region and propagated to the west. The errors of location make it difficult to determine the direction of rupture propagation for the second event, but this event too may have been started in the Perachora region. The aftershocks show a distinct clustering in the zones between the areas of rupture in the main event. They do not lie on a plane but in a volume in the hanging wall

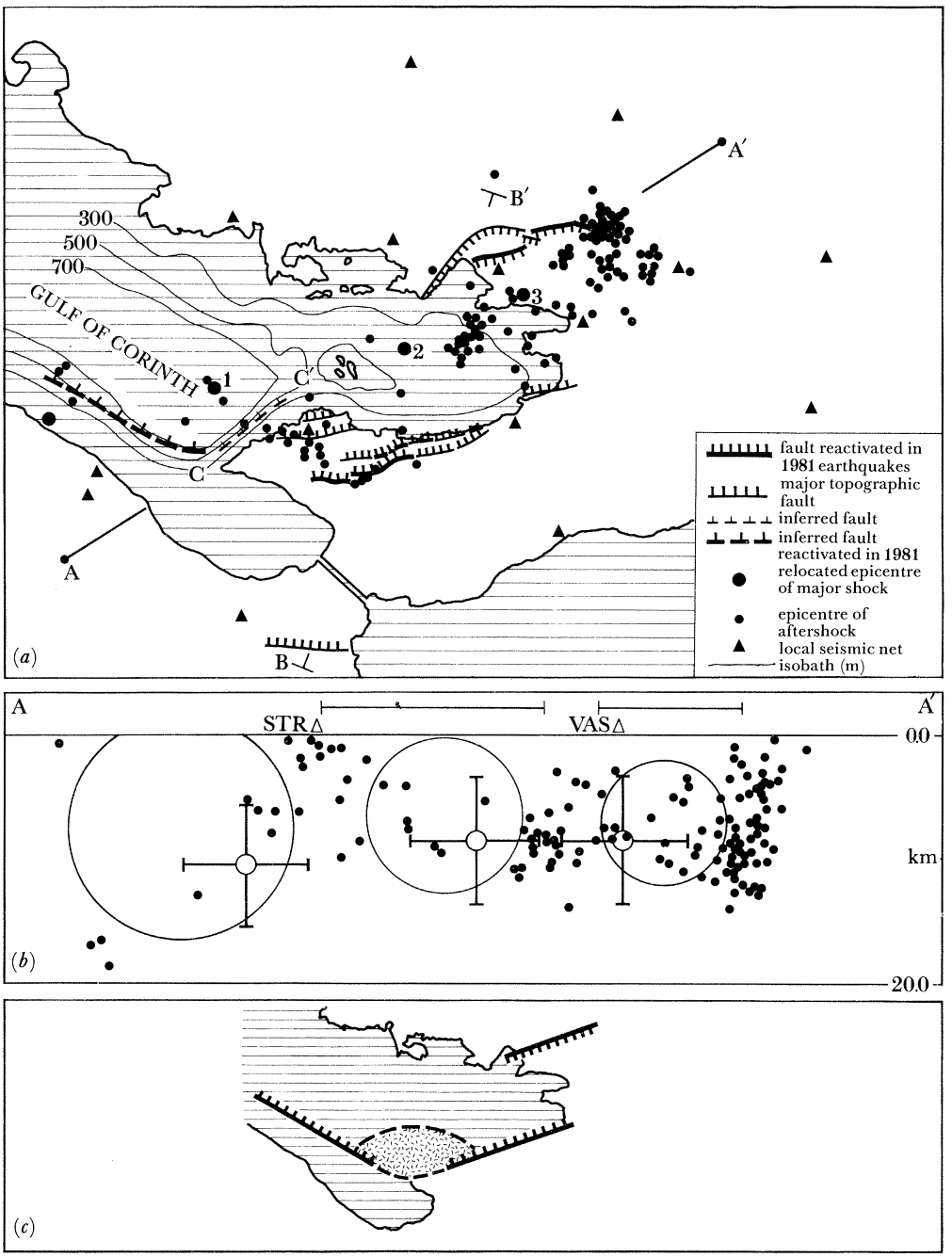

FIGURE 2. (*a*) Summary map showing the epicentres of the main events of the 1981 earthquakes: 24 February (1), 25 February (2) and 4 March (3). The smaller dots are aftershocks. AA′ indicates the section in (*b*). For a discussion of location accuracies see Jackson *et al.* (1982) and King *et al.* (1985). The broken line CC′ indicates a fault originally thought to have moved in the first event. The uplift data now show that it did not.

(*b*) Section AA′ shown in (*a*) with all events projected onto it. The locations of the main events whose positions were determined by the joint location method are indicated by small open circles with the corresponding error bars. The large circles are calculated from $M = 1.5 \times 10^{-3} \pi r^3$ where r is the radius and M the geometric moment (seismic moment divided by shear modulus) determined from long-period body waves (Jackson *et al.* 1982). The circles provide a guide to the area of faulting in the main events: they are positioned to enclose the hypocentre of their corresponding main shock and as few aftershocks as possible. A further discussion of this and the implications for the direction of rupture propagation may be found in King *et al.* (1985). The horizontal bars indicate the extent of surface faulting. STR and VAS are the two seismic stations closest to the section.

(*c*) A simplified map of the faults that moved in the 1981 earthquake sequence. The hatched region indicates the multiple faulting of the Perachora peninsula referred to later in the text.

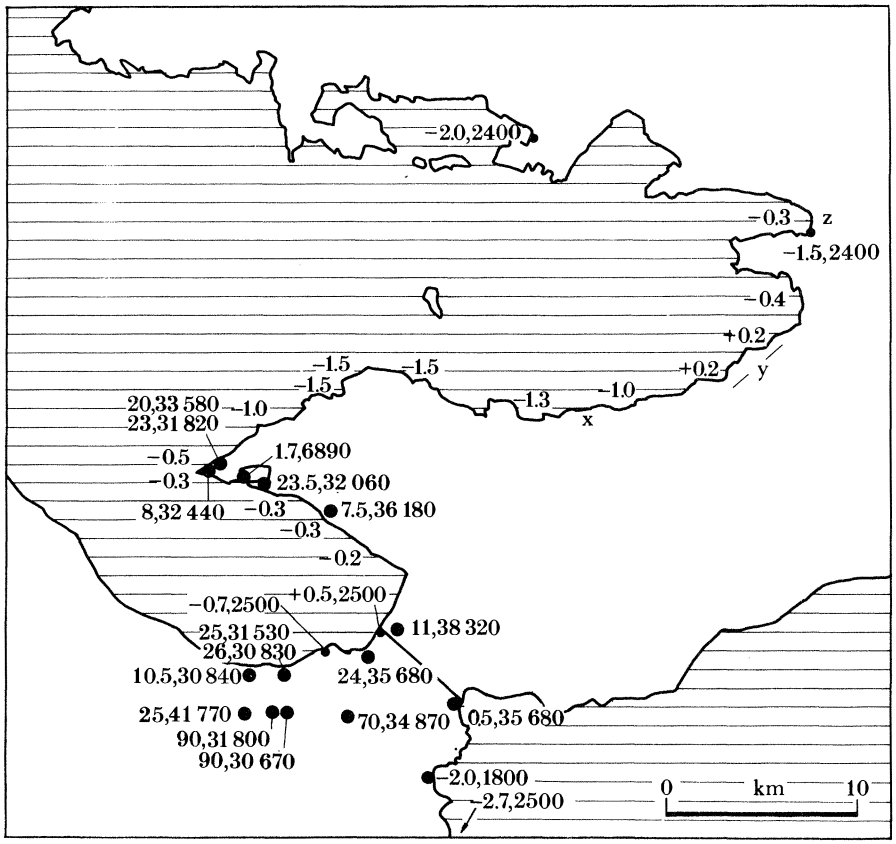

FIGURE 3. Location of sites for which emergence (positive) or submergence (negative), in metres, has been recorded since 1981; archaeological sites showing emergence or submergence in metres and approximate age in years (e.g. 2.7, 2000); and ^{14}C sampling sites showing present elevation in metres and age in years as in table 1 (e.g. 19, 31 530).

and therefore indicate movement on several faults. This style of deformation is apparent not only in the aftershocks but also in the Quaternary faulting of the Perachora region, where there is a complex system of minor faults with varying strikes and relatively small throws (figure 4*a*).

We suggest that, although the fault motion in the main earthquakes was relatively simple and confined to one surface to the east and one to the west of Perachora, the continuity of motion between the segments is distributed on many smaller faults.

The multiple faulting region is associated with a change of strike of the main faulting, a barrier in the sense of King & Yielding (1984). If the slip vector associated with the faulting also changes, the barrier is described as 'non-conservative' and gives rise to secondary faulting. The theoretical behaviour of such barriers is discussed by King (1984).

The Perachora faulting visible at the surface, however, is an indirect and not a direct manifestation of 'barrier' faulting at depth. Thus, before describing the Perachora and other regions in more detail we shall discuss the relations to be expected between superficial and deeper mechanical processes.

(*b*) *Earthquake faults and surface features*

Analysis of various earthquakes (King & Vita-Finzi 1981; King & Brewer 1983; King & Stein 1984) shows that fault motion at depth does not all reach the surface. Near-surface rocks

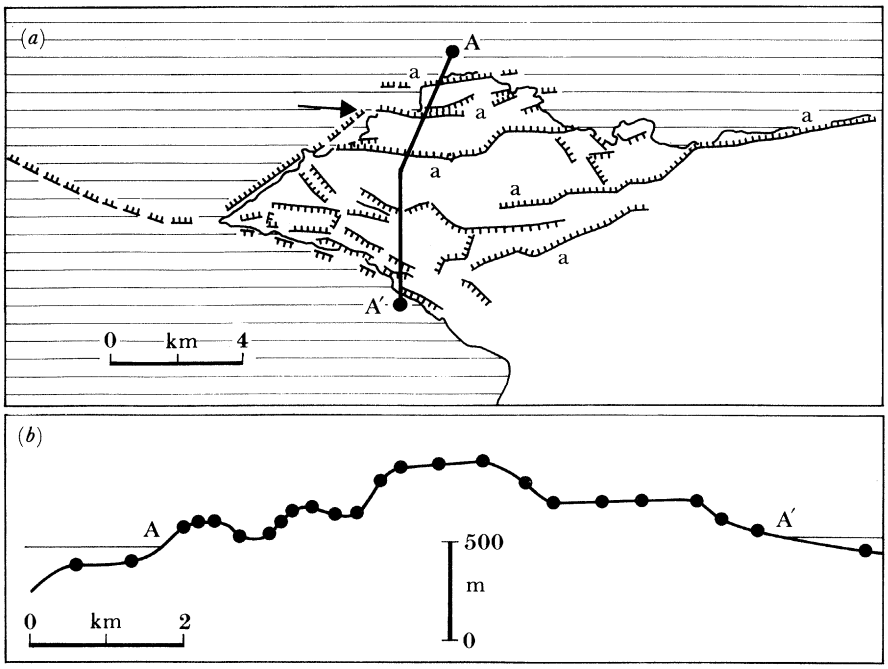

FIGURE 4. (*a*) Detailed fault map of the Perachora peninsula. The faults marked a are thought to be primary. Many of the others are secondary, for reasons given in the text. The position from which figure 9 (plate 1) was photographed is marked by an arrow. (*b*) Topographic section AA′ in (*a*). The dots indicate where heights were taken from the 1:50000 topographic map. The route of the section was chosen to avoid features that clearly existed in the pre-faulted landscape.

are stress-relieved on a scale of tens or hundreds of metres by stress corrosion on joints and fissures. Thus the rupture front at the time of an earthquake must be driven through this zone by fault motion at depth, and it is the consequent strains that accumulate to form folds and secondary faults. Although this is most readily observed in thrust environments, the same processes should occur in association with strike-slip and normal faulting. If we suppose that the surface zone is 1 km thick and the strain to failure in the rock is 10^{-3}, then 1 m of displacement along a primary fault will be lost in driving a fault to the surface. If the displacement at depth is 2 m, the surface rupture will be 1 m in amplitude; if 3 m, then a 2 m surface scarp will form and so forth. On this basis, an earthquake with less than 1 m of fault displacement at depth will not be associated with a primary surface break, the strain being manifested in the surface zone by folding and secondary faulting. One metre corresponds to magnitude (M_s) 6.0, the magnitude that divides events which normally have surface breaks from those which do not. The ratio of surface folding to surface faulting depends on the size of repeating events on the underlying faults.

A direct and important corollary of the foregoing discussion is that the surface expression of an earthquake or a repeated sequence of earthquakes does not scale with earthquake size. Since the size of events depends on the length of straight fault, long straight faults will produce surface scarps, whereas multiple short faults and hence barrier regions will produce surface folding and secondary faulting. Figure 5 illustrates some aspects of the deformation to be expected at a change in fault strike. Slip on the main fault plane becomes small or zero near the projected intersection of the two planes. It is taken up by the multiple faulting that creates

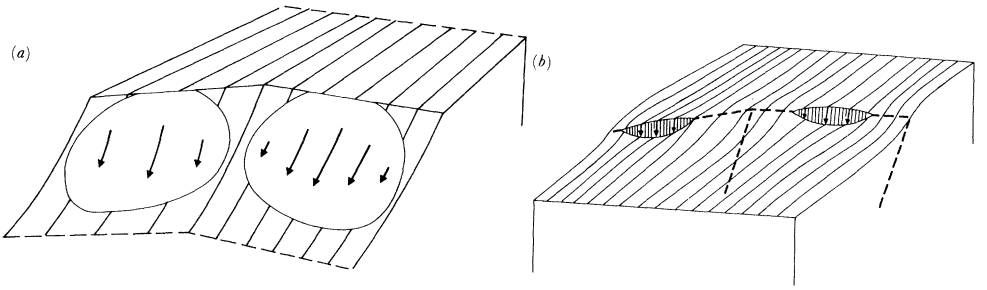

FIGURE 5. Diagrams illustrating the relation between the fault plane of the first and that of the second of the 1981 events. It is apparent that the two faults do not meet simply and that slip diminishes on each main fault as the projected line of intersection is approached. The motion between the two faults is taken up on a network of smaller faults (see figure 4). (The smaller faults are not shown in this block diagram.) The distribution of slip on the main faults is shown in (*a*), the general form of the surface deformation in (*b*).

aftershocks. At the surface, the main manifestation of this behaviour is downwarping rather than faulting. In the figure the slip vectors of the two main planes are shown to be parallel, in conformity with the fault plane solutions of Jackson *et al.* (1982). However, the auxiliary planes of these solutions were poorly constrained and the results of Dziewonski & Woodhouse (1983) and King *et al.* (1984) indicate a substantial difference in the slip vectors of the two events. Multiple faulting is made necessary by those components of slip that are not parallel to the line of intersection between the main fault planes (see King & Yielding 1984).

Figure 6 shows a sequence of idealized cross-sections for surface features above single and multiple faults. The sections on the left, (*a*)–(*c*), show deformation associated with a single fault that moves substantially in each earthquake. The sections on the right (*g*)–(*i*), are appropriate for a set of faults that move in many small earthquakes, and sections (*d*)–(*f*) for an intermediate case.

Two general features of the models should be noted. First, looking at each set of figures from top to bottom, we can see that the surface forms change qualitatively as the faults at depth grow and that they do not simply increase in size. Second, looking from left to right, we can see that the features associated with faults which grow by repeated small displacements never evolve to look like those which form as a result of a series of large increments of movement.

A feature shown in some of the sections is the development of secondary surface faults. We suggest that faults of this sort are completely different in nature from the major faults. The major faults are driven to the surface from depth and diminish in throw as they approach the surface. The secondary faults, on the other hand, start at the surface and propagate down. They are the consequence of large surface strains caused by motion on the main faults and the presence of near-surface irregularities on which rupture can initiate. Surface defects commonly control the strength of engineering materials and the same effect may be expected for the Earth's surface.

Secondary faults occur particularly where the main fault fails to reach the surface because it moves in repeated small increments. The surface material accommodates the deformation at depth with large strains and secondary faulting. The secondary faults are different from weak expressions of the main fault, and the belief that they should bear a simple kinematic relationship to the main faults at depth or to a regional stress field can create confusion. For example, estimates of regional stretching based on summing the displacements on secondary

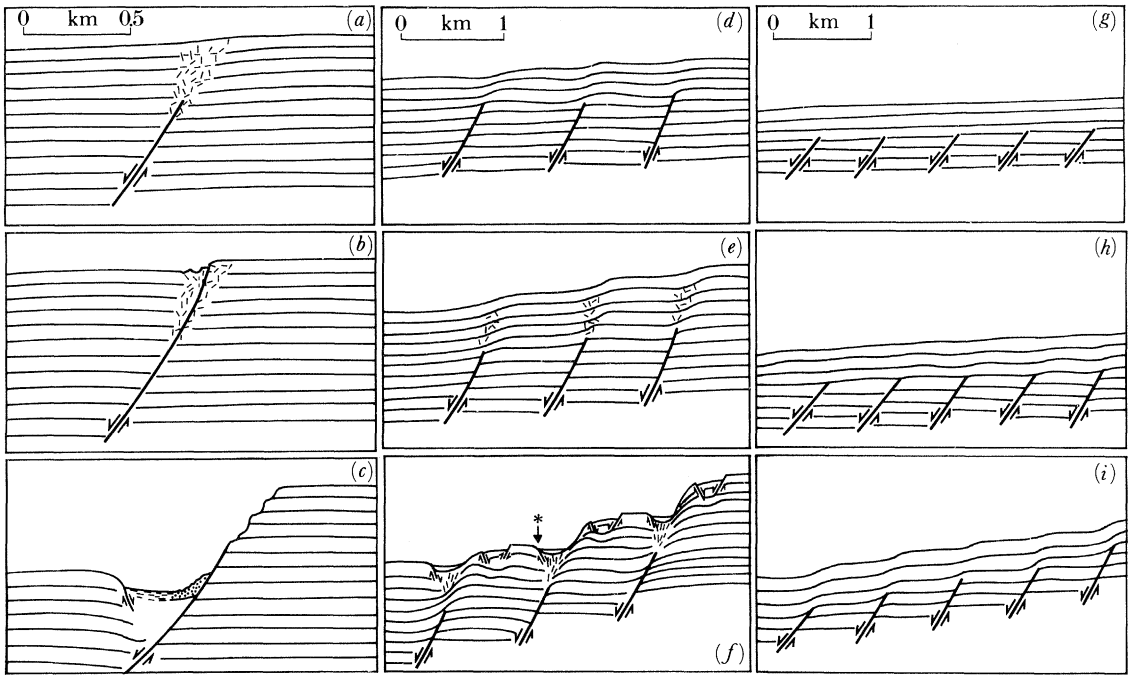

FIGURE 6. The evolution of surface features above faults that have earthquakes of different recurrent slip amplitudes. The diagrams are drawn for maximum clarity, and are not intended to be to scale. Furthermore, similar features occur on a range of scales. None the less, scale bars are added to indicate the approximate dimensions of the structures to be found in the Corinth area.

Sequence (*a*)–(*c*) is for a fault which experiences repeated events, each with substantially more than 1 m of displacement at depth. Early stages of evolution produce near-surface shattering and brecciation. (An excellent example of this, but outside our field area, is where the Athens–Thessaloniki motorway cuts through the Lochris faults.) Further motion on the fault at depth causes a fault surface to cut through the shattered material and it is this surface which finally forms a fault scarp. Slickensided surfaces in normal faults are commonly in recemented breccia. The diagrams indicate that the fault surface and the breccia are not contemporary although both are a consequence of motion of the same fault at depth. Greater motion on the same fault exposes the slickensided surface, (*c*), to leave a steep scarp which is ragged at the top and slickensided lower down. Antithetic faulting appears for large throws and is a consequence of the curvature of the fault plane. The near-surface curvature (upper 3 km nominally) is due to the variation of failure angle with depth and not to the processes that cause more profound dip changes at greater depth. Because the antithetic faults rupture down from the surface they form very clear features despite their small displacement.

Sequence (*d*)–(*f*) is for a set of three faults, each with repeat throws less, but not much less, than 1 m. Repeated fault motion of this amplitude can never cut the surface but is sufficiently large to produce extreme surface deformation. For small total fault throws, only surface folds appear, (*d*) and (*e*), but for larger throws secondary faults rupture down from the surface. They form very clear surface features but their kinematic relation to the main faulting is not simple.

Sequence (*g*)–(*i*) is for a set of five faults with repeat throws substantially less than 1 m. Motion on these faults creates downwarping. For small throws the surface downwarping is indistinguishable from a regional tilt. For large throws, (*i*), surface undulation becomes visible.

faulting is bound to result in an underestimate. The existence of secondary faulting is evidence that the surface rocks are experiencing large strains. The neat appearance of secondary faults and the consequent ease with which they can be mapped is a direct consequence of their mode of formation. Since they start from the surface, the secondary faults do not cut through their own debris. It may be that rift valleys have long been regarded as symmetrical structures because secondary antithetic faulting can have clear surface expression even if, in terms of deformation, it is not important. Only when the total throw on faults at each side of a graben, rather than their clarity, is considered does asymmetry become apparent.

(*c*) *Deformation in the Corinth region*

We mapped the structures in the Corinth region by identifying which of the features outlined in figure 6 had been responsible for the local morphology.

The maps that we develop (figures 7 and 8) are similar to fault maps but incorporate inferred subsurface faulting. Where the faulting is inferred, the usual symbol for normal faulting is replaced by an arrow symbol indicating observed surface downwarping. The usual symbol denotes faults of the kinds shown in figure 6*a–c*; the arrow symbol denotes deformation of the kind shown in figure 6*d–j*. Since the various structures grade into one another along strike, the choice of symbol is to some extent arbitrary. Clear examples of the various types can be found in the area and are now discussed in turn.

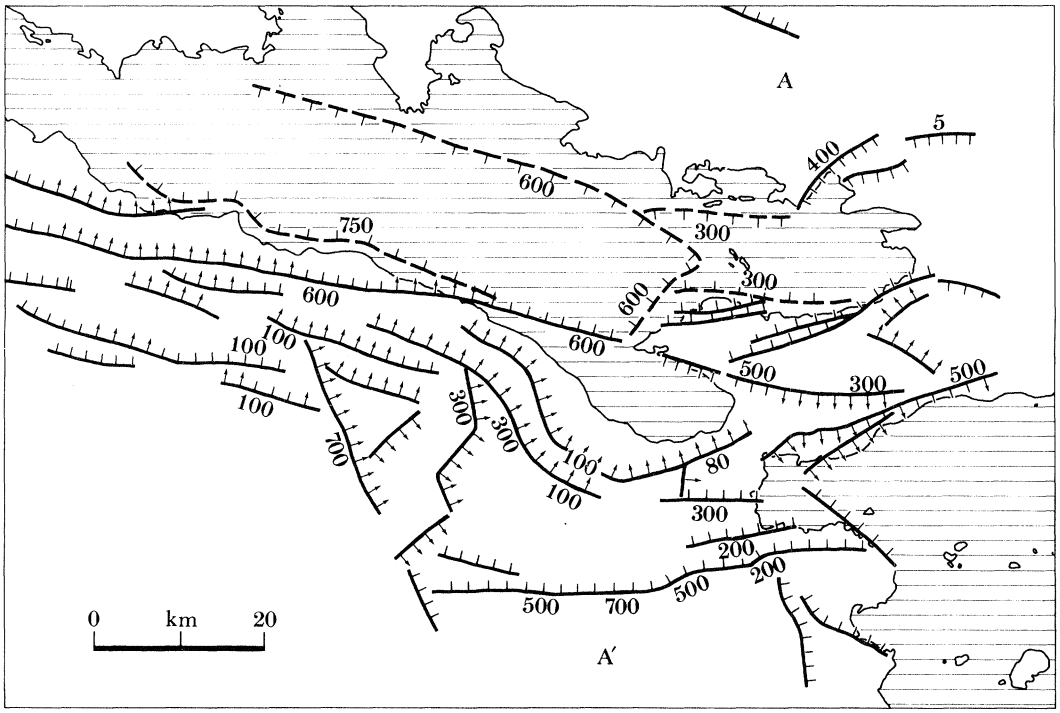

FIGURE 7. Faults and downwarps at the end of the Gulf of Corinth. Faults that approximate to those shown in figure 6*a–c* are indicated by the usual symbol for normal faulting. The arrow symbol indicates the other features in figure 6. Downwarp structures are readily identified in young soft-bedded rocks, whereas large scarps in similar material do not survive. Thus there can be a spurious relation between rock type and surface geology which may obscure the fact that the form of surface structures depends on the geometry of fault motion at depth and not on the rheology of near-surface rocks (see also King & Brewer 1983).

Undersea features are indicated as hypothetical faults in the absence of more information. The heights marked beside many of the features are the visible vertical throws estimated in the field with the aid of 1:50000 topographic maps. The numbers can only be regarded as a qualitative measure of the significance of the features since no allowance is made for sediment cover of the hanging wall. However, it is reassuring that summing these heights along many sections perpendicular to the overall strike of the faulting results in similar totals.

Some areas of the map (excluding the sea areas) are relatively free of faults. Although we examined some of these regions less carefully, the relative absence of faults is real.

The main linear fault scarps are unambiguous if ragged features. The faults between Perachora and Alepechori are good examples. The faults near Kaparelli in the north (see Jackson *et al.* 1982), however, are very different in character as they have a small total throw

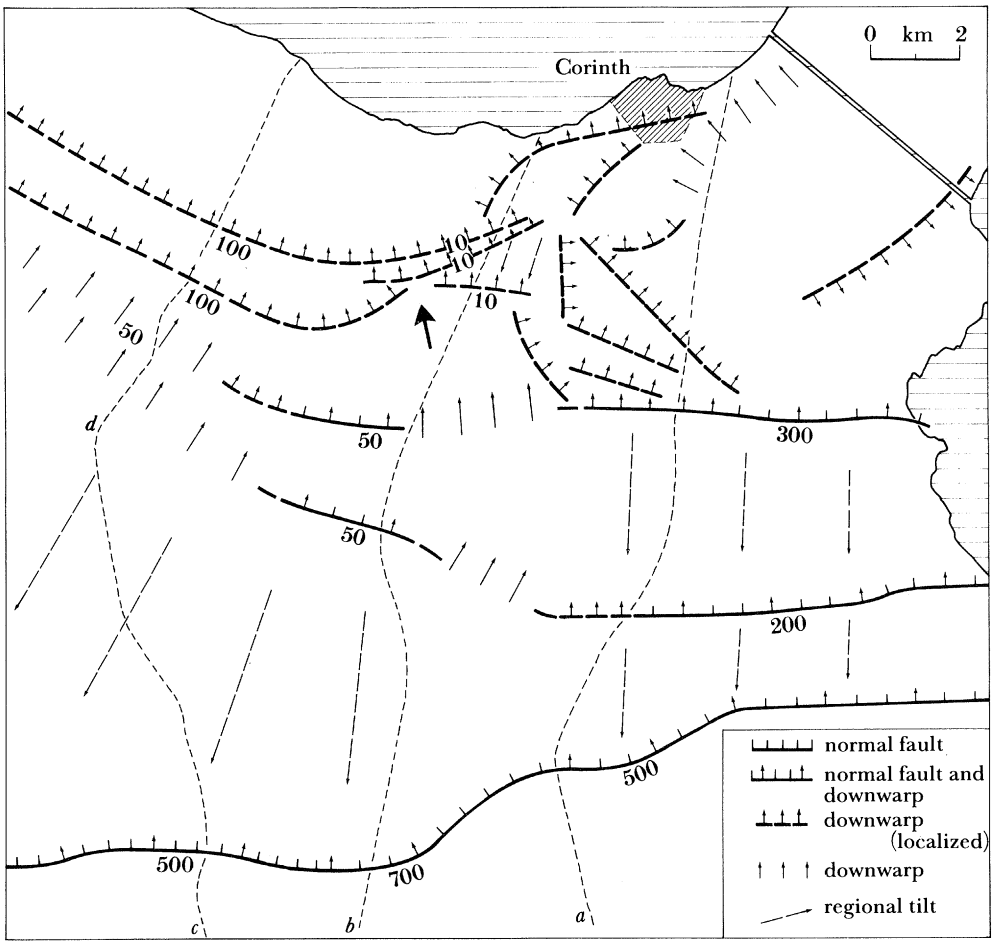

FIGURE 8. Faults, downwarps and back-tilting in the Corinth region. Numbers beside the features indicate their amplitude but no allowance is made for sediment infill, so that in many cases the total throw will be greater. The viewpoint of figure 11 is indicated by an arrow and d marks a place where the marls have a greater back-tilt than the present land surface. The dotted lines *a*–*c* indicate the cross sections in figure 10.

but a very clean morphological expression. They are apparently secondary or antithetic to the main fault. King *et al.* (1984) argue that they were initiated by rupture propagating downward.

The Perachora peninsula exhibits examples of the features shown in figure 6*d*–*f*. The surface manifestation of the faulting at depth is surface folding; the observed faulting is almost all secondary. Figure 4 shows a detailed map of this faulting. Because the region is mainly composed of unbedded massive limestone, the deformation is most readily traced by reference to landforms. The topographic section in figure 4*b*, for example, shows the major downwarp structures of the peninsula. The form of one of these is shown in figure 9 (plate 1), a photograph taken from a boat off a relatively inaccessible part of the area. The limestone is folded over towards the fault. Behind the warp structure is a small graben produced by stretching associated with the folding (figure 6*f*). Similar fold-related faults moved during the El Asnam earthquake (King & Vita-Finzi 1981). The features that can be seen in the photograph are sketched beneath it. In the sketch raised beaches are identified which are deformed in a similar way to the rocks themselves, though less markedly. The raised beaches disappear between the graben

faults. The upper of the two terraces is continuous with the raised beach at site 103 (see §3*b*) and is therefore probably about 30000 years old.

The feature in figure 9 is an example of one of the folds with secondary faults shown in figure 6*f*. The fold continues to the east and, whereas it is partially submerged where the photograph is taken, it rises fully above sea level at Milokopi. After the earthquake a small amount of secondary faulting was observed at the surface here; its position is marked by an asterisk in figure 6*f*.

Faulting and fault-related folding occur in the area around and to the east and west of Corinth city (figures 7 and 8). Many of the morphological features that we show as fault-related folds have long been regarded as marine terraces (see Sébrier (1977) for a historical review) but they posed problems to those investigators who sought to interpret them in this way. In particular, as they changed height along strike, complex local tilting was required to explain their present varying slope. No explanation for such tilting is available, whereas the mechanisms that we propose account for them very simply and, as we shall see, the evidence for marine influence above 200 m is not clear. (This should not be confused with evidence for earlier high-level brackish lakes.)

Near the coast, downwarp folds become associated with former sea levels and abandoned cliff lines but the escarpments were not formed by wave action alone. The point is well illustrated by the feature known as the Temple Terrace (Sébrier 1977). At ancient Corinth it is clearly associated with marine deposits; traced westwards it climbs steadily from 70 to 100 m and loses its marine character. Contemporary fault scarps and downwarps which change along strike from dividing one continental environment from another to separating continental from marine environments are common, as we have already noted. The feature shown in figure 9 is one local example.

Some important features of the region near Corinth city can be illustrated by using the three topographic sections in figure 10. Their locations may be found by referring to the map in figure 8. The first section (figure 10*a*) is for the region where three major faults approach from the east. The central fault has a small throw where it crosses the section, and a kilometre to the west it becomes a downwarp. Near the sea, further east, it is a substantial fault. The topography in the region of the first section is thus largely dominated by faults.

This is not true for the second section (figure 10*b*), which crosses three peaks (including Acrocorinth) that predate the faulting. In the field the major scarps that are associated with Quaternary or recent fault motion can readily be identified by the angular nature of their surfaces and scree mantles compared to the equally steep but rounded and weathered outcrops of features such as Acrocorinth (figure 11, plate 1). In other words topographic sections and maps are of limited value.

The third section (figure 10*c*) passes through a region which had no substantial pre-fault topography and is composed of marls capped by a layer of continental (mainly fluvial or lake-margin) sands and gravels between 1 and 5 m thick. The marls are conformable with this 'caprock', which directly underlies the present land surface where that surface is not cut by active badland erosion. The form of the land surface therefore give a good indication of the extent of warping and thus of subsurface faulting (figure 12, plate 1). We presume that the marls represent deposits from an inland lake that existed before the Gulf of Corinth deepened sufficiently to permit access by the sea (see Depéret 1913). The 'caprock' represents terrestrial material which transgressed across the lake bed as its level progressively dropped. This

PHILOSOPHICAL TRANSACTIONS OF THE ROYAL SOCIETY A MATHEMATICAL, PHYSICAL & ENGINEERING SCIENCES

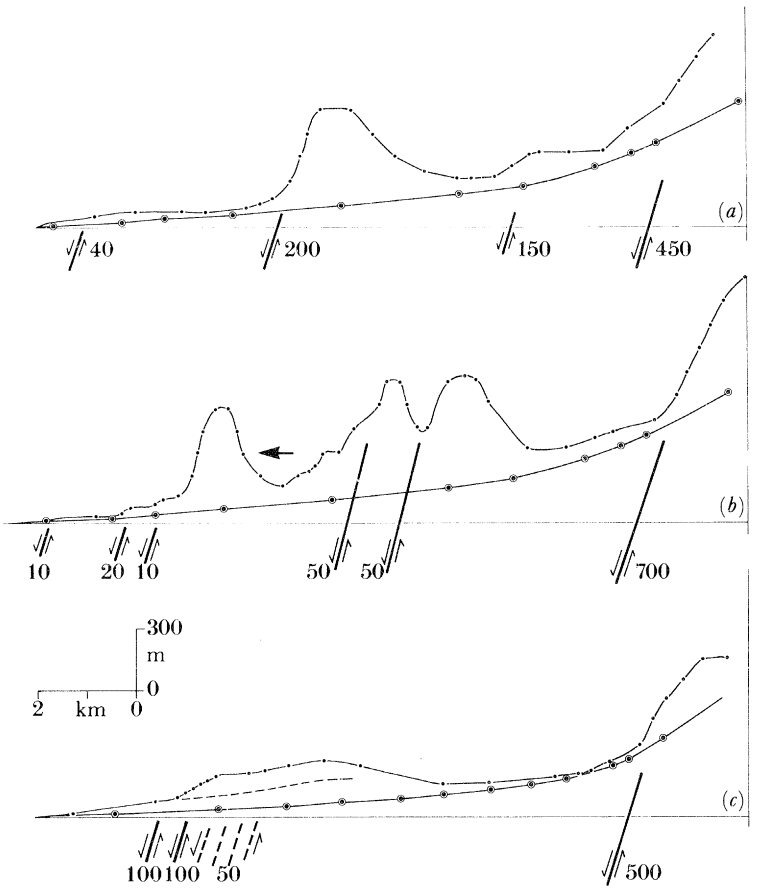

FIGURE 10. Topographic sections corresponding to *a*, *b* and *c* in figure 8. The river profiles in (*a*) and (*b*), indicated by a line joining a series of circles, are provided by a river that follows a course between (*a*) and (*b*); the river in (*c*) lies between (*b*) and (*c*). In sections (*a*) and (*c*) the landforms are largely fault-controlled although the number of faults and hence the form of the surface deformation are very different. In (*c*) a broken line indicates a lower-level erosion surface in the river valley, presumably formed at an intermediate stage of development of the fault system. Section (*b*) is through the limestone mass of Acrocorinth, about 1 km south of the site of Ancient Corinth, and similar features to the south of it. These features existed in the topography before the formation of the fault system and were never covered by marl. They stand above the topography produced by the current fault system. Figure 11 is taken in the direction and from the position indicated in (*b*) and in figure 8 by arrows.

evolution is shown schematically in figure 13. The earlier part of this scheme can be recognized at present at the edge of the Great Salt Lake in Utah.

The downwarp structures which the last of the three sections (figure 10*c*) crosses are indicated on the map as curving along strike. More probably they consist at depth of a series of short segments. Whatever their detailed geometry, the changes of strike will prevent large earthquakes and hence the development of surface faulting. There is one important item of evidence to suggest that the differences between the three sections are not primarily influenced by lithology or stratigraphy. The marls and caprock can be traced right up to the massive limestone block of Acrocorinth and may be seen from the access road. They are folded and warped in such a way that the limestone must be similarly deformed, although the deformation cannot readily be detected. If the surface deformation style was primarily controlled by rock type and not the geometry of faulting at depth, then the Acrocorinth block and thin superficial sediments

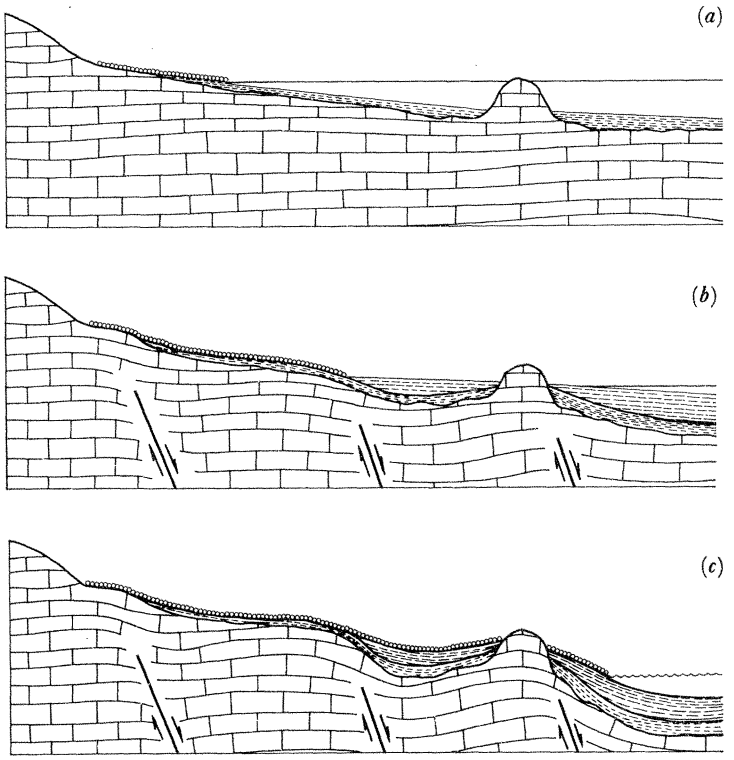

FIGURE 13. Schematic sections showing evolution of coastal sedimentary environments in the eastern Gulf of Corinth. The sections run roughly N–S, with S on the left. (*a*) Marls are deposited in the bed of a brackish lake. Some features protrude as islands, Acrocorinth being one example. The lake shore marks the boundary between marls and continental deposits. (*b*) Faulting causes the lake bed and land surface to drop. The continental deposits that are to become the present-day caprock transgress conformably over the lake deposits. Deformation of the early lake deposits causes unconformities to appear within the marls. (*c*) Continued faulting lets in the sea and in due course the resulting uplift produces raised beaches. Note the deformation undergone by the bedrock 'island' equated above with Acrocorinth.

would be faulted and not folded. The configuration of limestone and sediments can be seen in figure 11. The gound surface corresponds to 'caprock' where it has not been modified by erosion.

Each of the topographic sections in figure 10*a–c* can be compared with the profile of the nearest two rivers plotted on the same scale and on the same axes. Neither of the river profiles departs from a smooth curve at the level of resolution used here. Thus activity on any of the structures that they traverse must have been relatively low for some time, an inference which supports our later conclusion that the fault systems south of the city of Corinth are relatively inactive. The rivers do not exhibit clear terraces which could serve to date downcutting. An intermediate-level erosion surface can be seen and is shown in figure 10*c*, but its height is variable and we could find no way to date it.

Although the faulting in the north (figure 8) loses its surface expression eastwards to appear as downwarping, the southern fault appears as a fault over much of its length. This may be due to lack of sediment cover, its relative linearity, or both.

The most striking downwarp features in the region are found in the region of Kiaton. The cross section in figure 14 is along the Kiaton to Souli road (see figure 1), which cuts across the strike of the structures. Driving up this road one gains the impression of a series of

PHILOSOPHICAL TRANSACTIONS OF THE ROYAL SOCIETY A MATHEMATICAL, PHYSICAL & ENGINEERING SCIENCES

benches although the topographic section suggests a smoother gradient. The region is again composed of marl surmounted by caprock, with the latter becoming coarser and thicker with increasing altitude, presumably as the sediment source is approached. The caprock is again conformable with the land surface. Figure 15 (plate 1) shows caprock and marl folded over the feature marked A in figure 14.

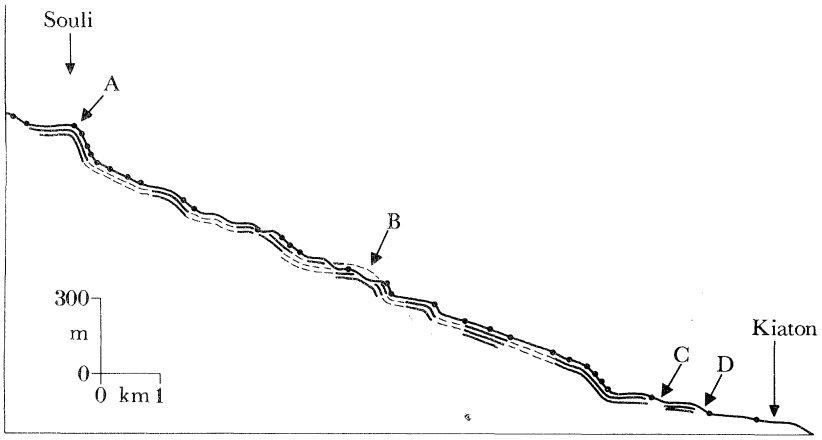

FIGURE 14. Topographic section south of Kiaton (compare with figure 6*g–i*). The dots indicate heights taken from 1:50000 topographic maps. The intermediate heights were estimated in the field. Bedding is indicated in the section and is almost everywhere conformable with the land surface. The rocks are marls surmounted by a cemented gravel (caprock), which in some places forms the land surface and in others is covered by a thin soil. A photograph taken at A in the section is shown in figure 15. The only places where the caprock and land surface are not conformable is at B, where the surface has been cut by post-deformational river erosion, and at C and D, where there are collapsed marine cliffs. The feature illustrated is largely a downwarp with benches in it. The higher benches, as well as those lower down, have been previously identified as raised beaches. However, all except C and D change altitude and amplitude incoherently along strike and the abundant evidence of beach environments in C and D is absent at the higher levels.

DESCRIPTION OF PLATE 1

FIGURE 9. View east in the direction of the arrow in figure 4. The sketch indicates the main structural features, including a deformed raised beach. Level A appears to correspond to the terrace at site 103 (table 1, figure 19 (plate 2)).

FIGURE 11. View north in the direction of the arrow in figure 8 and figure 10*d*. Acrocorinth (right) was an outcrop of limestone protruding through the marls and caprock of the pre-faulting erosion surface. The marls are now subject to badland erosion resulting from backtilting and a drop of river level due to faulting between Acrocorinth and the sea. The marls and caprock are folded, requiring similar deformation of the limestone of Acrocorinth.

FIGURE 12. A view north along the river valley between sections *b* and *c* of figure 8. Note the caprock (upper left), which is conformable with the uneroded land surface and the marl beneath. It is this conformable relationship which makes it possible to use topographic sections for determining the deformation of the underlying strata resulting from buried faults.

FIGURE 15. Folding of the caprock over a buried fault on the Kiaton road (see A in figure 14). The caprock is composed of sands and gravels of continental origin. In some places it is clearly fluviatile. In general the composition is coarser and the caprock thicker (up to 3 m) near the hills, and it becomes finer and thinner near the coast where it is also mixed with beach deposits. The caprock results from the transgression of debris from the adjacent mountains over the marls as the sea or lake in which they were deposited retreated. In some places (including this location) marls are interbedded with the caprock near the surface indicating that the retreat was not monotonic. Caprock covers the marls and is conformable with the land surface except where it has been removed by badland erosion or where limestone outcrops rise above the old lake surface (see figure 11).

PHILOSOPHICAL TRANSACTIONS OF THE ROYAL SOCIETY A MATHEMATICAL, PHYSICAL & ENGINEERING SCIENCES

9

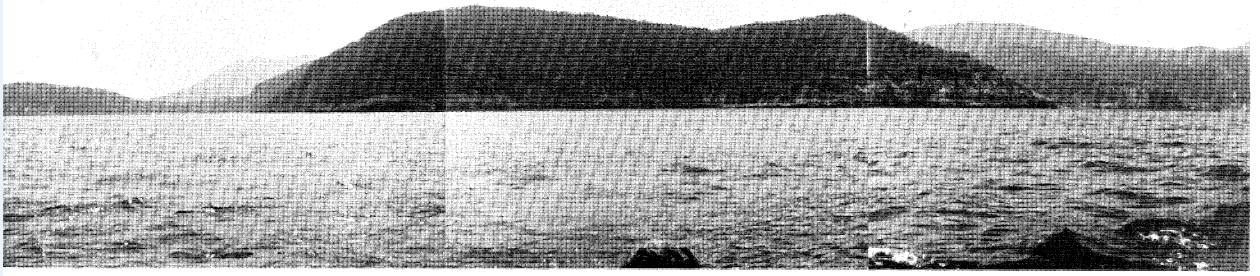

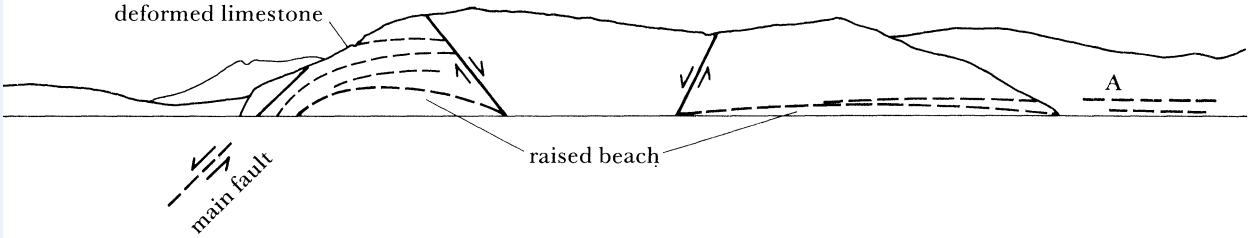

11

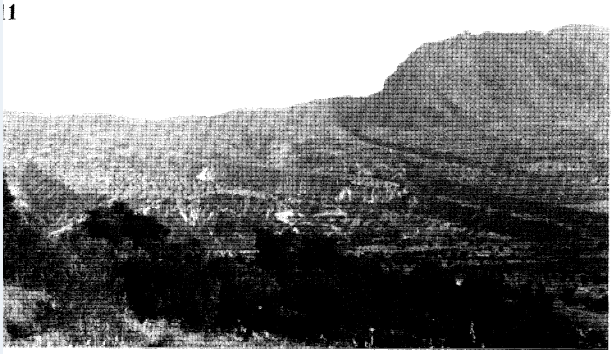

12

5

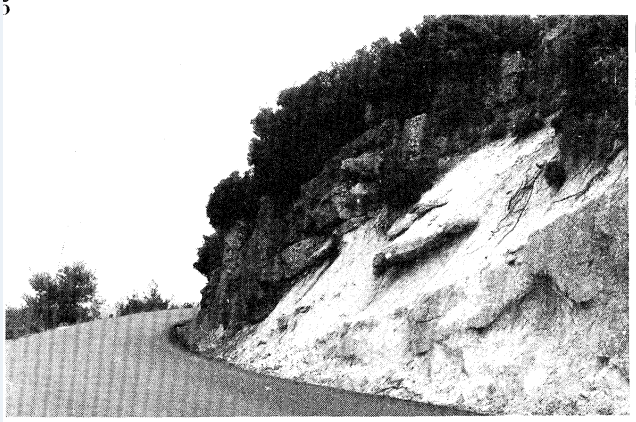

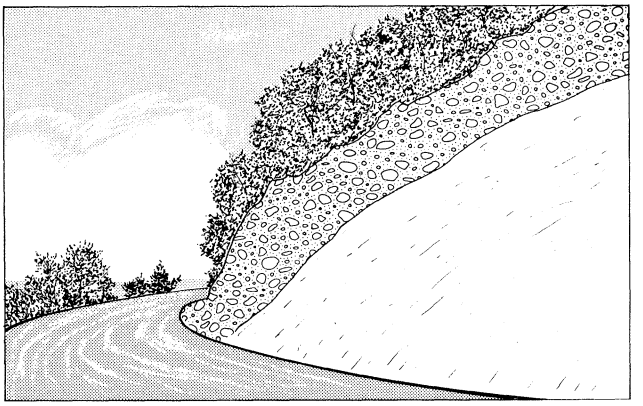

FIGURES 9, 11, 12 AND 15. For description see opposite.

(*Facing p.* 394)

PHILOSOPHICAL TRANSACTIONS OF THE ROYAL SOCIETY A MATHEMATICAL, PHYSICAL & ENGINEERING SCIENCES

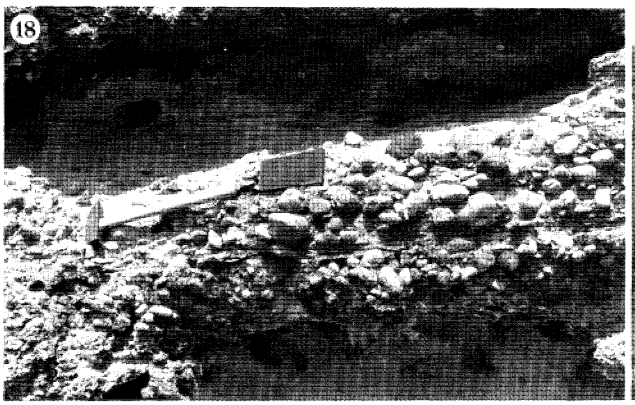

FIGURES 16–21. For description see opposite.

PHILOSOPHICAL TRANSACTIONS OF THE ROYAL SOCIETY A MATHEMATICAL, PHYSICAL & ENGINEERING SCIENCES

The Kiaton region is associated with a major change of fault strike and is an example of faults evolving in the manner shown in figure 6*g–i*.

(*d*) *Discussion*

In the earthquake of 1981 new faulting appeared at the base of major fault escarpments and it was evident that repeated similar events could account for the observed morphology. When we attempted to map the continuation of these structures we found that their character changed. The nature of the observed surface features can be explained on the basis of a plausible model in which multiple faulting at depth occurs where major faults change strike.

Using the models as a guide we have made maps intended to reflect the likely configuration of subsurface structures. On the maps we show the size of the surface features in metres. The values are approximate but since the features in the map vary in vertical relief and hence tectonic significance by more than a factor of one hundred such information is still useful. The figures do not represent total throw on presumed buried faults because of sediment infill.

None the less, by adding the throws on any north–south section across the southern edge of the eastern Gulf of Corinth, it can be seen that the total vertical throw is roughly independent of whether the structures which are crossed are faults or downwarps.

The structural maps that we develop provide a basis on which to discuss the evolution of the Gulf using information about earlier sea-level heights. The model that we adopt in §5 to discuss chronology is two-dimensional, like that of Jackson *et al.* (1982). More faults are introduced, however, to form fault zones and these modify the simple behaviour of the earlier scheme.

3. Chronology

The presence of numerous archaeological sites in the area offered the promise of data bearing on the historic and prehistoric periods. In addition it was hoped that some of the marine terraces would prove to be datable and hence furnish an indication of movements before the time of human occupation. Two uranium-series ages have been determined on the fossil beaches of the Corinth area but they are regarded as unreliable (Sébrier 1977). The 'New Corinth' terrace gave a date of 49000 ± 20000 years but as the terrace had been ascribed to the Tyrrhenian

---

Description of plate 2

Figure 16. Beachrock overlying the ramp used to drag boats across the Isthmus of Corinth in antiquity. The upper surface of the beach rock is about 0.5 m above present high water. The beachrock is certainly younger and possibly much younger than the ramp.

Figure 17. A view of site 103b from the sea. The upper beds are marine in origin and overlie the marls unconformably. An unconformable contact is usual between these deposits, whereas the contact between caprock and marl is apparently always conformable.

Figure 18. Pebbles of the beach deposit at site 501. Identification of features such as this containing datable material enables the former waterline to be established to within 1 m.

Figure 19. Escarpment near site 2 (figure 3, table 1). Note the angular unconformity between the Pleistocene marine deposits and the underlying marl.

Figure 20. Caprock gravels conformably overlying marls and unconformably covered by beach gravels at site 2. The hammer indicates the unconformity.

Figure 21. Scanning electronmicrograph of *Pinna fragilis* from site 302 showing calcitic prisms of outer shell layer. Note that all contamination is on the surface (lower left) and was therefore removed before dating. Scale bar represents 100 μm.

PHILOSOPHICAL TRANSACTIONS OF THE ROYAL SOCIETY A MATHEMATICAL, PHYSICAL & ENGINEERING SCIENCES

marine stage of the Pleistocene, which had come to a close about 75000 years B.P., the U-series age was considered to be too low. The 'Old Corinth' terrace gave a date of 235000^{+40000}_{-30000} years but it was viewed as more probably of 'Milazzian' age and hence over one million years old. In the absence of data on sample quality (Ivanovich *et al.* 1973) any proper assessment of either date is difficult but the 'New Corinth' result is not inconsistent with the ^{14}C ages reported here. The total absence of ^{14}C ages appears to stem from the general acceptance of a Tyrrhenian or older age for the area's post-Tertiary terraces on the basis of their fossil content, for it made any attempt at dating by the radiocarbon method appear futile. Although the number of marine transgressions encompassed by the Tyrrhenian is a matter for dispute, there is general agreement that its oldest manifestation ('Tyrrhenian I' or 'Palaeotyrrhenian') is over 200000 years old, that the Eutyrrhenian (Tyrrhenian II) with its *Strombus latus* (= *bubonius*) fauna dates from 124000 ± 10000 years ago, and that the youngest Tyrrhenian (III) dates from the late Eem, that is about 75000–90000 years ago (West 1968). The radiocarbon method is of course restricted to the last 50000 years or thereabouts.

Even so, an attempt to date some of the beaches by ^{14}C seemed to be justified. Not all the beaches had yielded diagnostic Tyrrhenian fossils, and more importantly the chronology of these fossils was open to question, especially as the radiometric ages for the Tyrrhenian elsewhere in the Mediterranean were of dubious validity (Stearns & Thurber 1967). Finally, the conventional view that raised beaches date from interglacial periods was more than usually suspect in an area with a lively tectonic history.

(*a*) *Archaeological evidence*

The Saronic Gulf

The displacement of ancient harbours and quarries relative to sea level in the Mediterranean has been investigated by Flemming (1978). Two of his sites fall within this area; *Cenchreae* (Kenchreai), and *Epidauros* (Palia Epidauros), 30 km further south. *Cenchreae* indicates submergence by 2 m, and *Epidauros* by 2.7 m. Most of the submergence at *Cenchreae* took place after the Augustan period (Scranton & Ramage 1967).

Corinth and the Isthmus of Corinth

At the northern entrance of the Corinth Canal there are the remnants of the ramp (*diolkos*) that preceded the canal as a route across the isthmus (Isthmia). The northernmost part of the ramp is covered by beachrock to a maximum of 0.5 m above present high water (figure 16, plate 2). Emergence evidently postdates construction of the ramp, which probably took place in the fifth century BC (Papahatzis 1981). The ramp doubtless extended into the sea, and as the beachrock could have formed below high water, the total emergence has exceeded 0.5 m. *Lechaeum* (Lechaion), the ancient harbour of Corinth 1 km west of the modern town, is submerged by 0.7 m (Flemming 1978).

The Perachora Peninsula

An important site in the centre of our study area is the partially submerged Helladic settlement of the third millennium BC on the narrow neck of land between the Vouliegmeni (translation: submerged) lagoon and the sea (Fossey 1969). A canal now cuts through the neck. According to Payne *et al.* (1940) it was excavated in the late nineteenth century. They based their statement on the evidence of one old man of nearly seventy, who had observed digging

in progress when young and assumed that a new canal was being made. Yet there is ample evidence for a much earlier marine connection. The Helladic site shows that submergence followed or perhaps helped to end occupation. The position of a jetty of uncertain age at the Heraion (Perachora) indicates about 1 m of emergence.

The northern Gulf of Corinth

Since the fourth century BC the sea has encroached on the land by about 1.5 m at *Aegosthena* (Porto Germano) and by about 2 m at *Siphai* (Aliki) (Benson 1895; Schwandner 1977; R. Tomlinson, personal communication).

(*b*) *Radiometric dating*

Molluscs intended for ^{14}C dating were inspected in thin section by using acetate peels and analysed by X-ray diffraction to ensure that their original mineralogy was unchanged and that all surface contamination had been removed (Vita-Finzi 1980). When doubts persisted, notably with specimens of mixed mineralogy, scanning electron microscopy was also used. The samples came from shallow-water and beach deposits (figures 17 and 18, plate 2).

Ancient Corinth

Near Ancient Corinth, terrace fragments are exposed at different elevations in natural sections, quarries and roadcuts. The feature termed the Old Corinth terrace by previous workers and exposed by the new Argos road was sampled for dating at two locations. At site B2/101 the shells in question were obtained from a beach series 1.5 m thick, which rests on cemented sands and is in turn overlain by 1.5 m of sands; ^{14}C dating indicates some 90 m of emergence in the last 30000 years. At site B6/103 the beach, here 30 cm thick, is overlain by 2 m of cemented gravels and rests unconformably on marls. Emergence, again by 90 m, dates from the last 32000 years. Site 701 is a quarry face in the same terrace. It provided an articulated specimen of *Mytilus*. Further east, at site 914, a fossiliferous bed of fine gravel 1.5 m thick and rich in *Crassostrea* and *Pinna* is overlaid by 8 m of sands whose upper surface forms a well defined terrace. Emergence here amounts to a minimum of 25 m in the last 42000 years.

Corinth

Site 2 (figure 19, plate 2) is close to the type locality for the 'New Corinth' terrace of Dufaure *et al.* (1975) and profile Ie of Freyberg (1973). The sequence includes three main units. The uppermost consists of 10 m of dune sands interbedded with red colluvium, presumably the local equivalent of the regressive Kokkinopilos beds of northwest Greece (Vita-Finzi 1978). These overlie 4 m of grey cemented sand, which in turn rests on 2.5 m of white marls displaying vertical burrows and a basal gravel.

Sample 2a was collected at a depth of 1 m in the grey sands *ca.* 25 m above sea level. It consists of *Cerastoderma glaucum* in growth position. Other molluscs in the sands include *Arca noae* (with more specimens of *C. glaucum*) near the contact with the dune sands, and *Dosinia* sp., *Callista chione*, *Conus ventricosus*, *Venus verrucosa*, *Spondylus gaederopus*, *Cerithium vulgatum*, *Loripes lacteus* and *Crassostrea* further down the section. The marls contain articulated specimens of *Dosinia* sp. and *Mytilus galloprovincialis*. The basal gravels are rich in *Crassostrea* and *Pecten*. The stratigraphy and fauna suggest gradual deepening after the gravelly beach had formed about 31500 years ago. Finally, rapid emergence by 25 m was accompanied by accumulation of the dune series.

PHILOSOPHICAL TRANSACTIONS OF THE ROYAL SOCIETY A MATHEMATICAL, PHYSICAL & ENGINEERING SCIENCES

The second sample (3c) came from 1 m higher in the section, and confirms the chronology, as it is a little younger than sample 2a. About 150 m further along the escarpment the sequence includes only 3 m of dunes and colluvial lenses, 2 m of sand (with *M. galloprovincialis*) and 70 cm of grey marl with a few pebbles and cobbles at the base and containing numerous specimens of *Crassostrea* and *Pecten*, but these sections have not yet been dated.

At site 2 the sands and gravels rest unconformably on well bedded marls, which are capped unconformably by some 80 cm of pebbles with a hint of imbrication towards the northwest. The unconformity between the pebbles and the overlying beach gravels is not immediately apparent (figure 20, plate 2). Sébrier (1977) recognizes a single pebbly horizon (layer b) separated by an unconformity from the overlying marls and by an angular unconformity from those below. Freyberg (1973) and Keraudren (1970–2) favour a similar view. The interpretation given here shows that the beach sequence developed over the basal marls, which in places happen to be capped by cemented gravels. The 'Tchaudian' fauna reported by Sébrier (1977) from the caprock is thus of no relevance to the ecology and age of the overlying fossil beach.

A similar terrace level can be identified east of Corinth, where cultivation has exposed about 2 m of fossiliferous gravels and sands resting unconformably on a marl series (site 913). The age of these sands, which is identical with that of site 5, is not inconsistent with the ages obtained at site 2, and indicates 24 m of emergence in the last 36000 years. To the west the terrace falls in height, and the base of the beach deposits, which is 19 m above high water at site 2, is 8.5 m lower at site 912, south of the ancient harbour of *Lechaeum*. Here 20 cm of cemented cobbles and pebbles in a sandy matrix overlie 1 m of fossiliferous sands. The sequence rates on flat-bedded marls. The dated sample of *V. verrucosa* came from halfway down the sand. It was associated with *A. noae*, *C. chione*, *Chama*, *L. lacteus*, *C. glaucum* (still articulated), *C. vulgatum*, *Crassostrea* and coral fragments, for which shallow sublittoral conditions may be inferred. Emergence has amounted to 10.5 m in 31000 years.

The Isthmus of Corinth

Ten ^{14}C ages have now been obtained for the southeastern shore of the Gulf. Two of them are on shells from the Pleistocene beds cut by the Corinth Canal.

Site 302 is on the northeastern bank of the Canal about 2 km south of the coast. The sample of *Pinna fragilis* came from a grey sand overlain by 1.5 m of conglomerates and 7 m of weakly cemented sands. According to Freyberg (1973) the grey sand (*Gelbsand* or yellow sand in his terminology) dates from Tyrrhenian I (Palaeotyrrhenian) times. His sections indicate a height of about 12 m above sea level for the sample site. The deposit also contains *A. noae*, *C. glaucum*, *L. lacteus*, *Lutraria* sp., still articulated and sometimes in growth position, *Natica*, *Tellina*, *Glycymeris glycymeris*, *Ostrea edulis* and *Chama*. Freyberg (1973) reports *Pecten* and *Pectunculus* as well as *Pinna* sp. The dated material evidently does not point unambiguously to a particular depth of water but the assemblage is most readily explained by deposition at a depth of 2–5 m; thus emergence in the last 38000 years totals about 13–16 m. Site 5 is on the west bank at the southern end of the Canal, where an oyster bed at least 1 m thick (which supplied the sample) is separated by a weak unconformity from an overlying red colluvium. The age obtained on the *Crassostrea* sample thus refers to a shoreline not long before its emergence and hence indicates a minimum of 0.5 m of emergence in the last 36000 years.

The Perachora Peninsula

Two independent determinations on *Notirus irus* from borings in limestone blocks exposed in the canal banks at Vouliegmeni at a height of 1.7 m gave an age of *ca.* 7000 years (table 1). The presence of specimens of *Hydrobia* and *M. galloprovincialis* as well as *N. irus* points to shallow sublittoral conditions, and hence could indicate emergence by more than the 1.7 m required for purely intertidal fauna. A value of 3 m appears reasonable.

Of the other sites on the peninsula with molluscan borings, only one – 502 – yielded bivalves still within the holes (in this case *Lithophaga*) and the shells were too badly altered to serve for ^{14}C analysis. Dating of the ancient waterline at this site is still possible, however, because the *Lithophaga* level, which is associated with a vermetid reef and a *Crassostrea* bank, is immediately underlain by a sandy bed rich in *A. noae* (of which a few individuals are still articulated), *C. vulgatum* and other indicators of shallow sublittoral conditions. The water level to which the ^{14}C date of 32000 years refers was thus about 23.5 m above present high water, but a cemented reef, rich in shallower water species such as *Pecten* and *Turritella communis* and 5 m higher, points to greater submergence at an earlier stage by at least an additional 10 m and thus later emergence by some 33 m. Herforth & Richter (1979) describe marine terraces in the vicinity at several distinct heights up to 100 m.

Palaeotyrrhenian faunas have been reported elsewhere on the peninsula. According to Richter *et al.* (1979), a marine terrace of Palaeotyrrhenian age overlies a series of reef bioherms at a height of about 20 m to the north of Cape Heraion. Site 103b of the present paper (figure 17, plate 2) corresponds to the section described by these authors, with a pebbly beach deposit containing a death assemblage of *A. noae*, *C. vulgatum*, *Gibbula magus*, *Bittium reticulatum*, *Crassostrea* and other shallow sublittoral species. Over 23 m of emergence is suggested in the last 32000 years. Site 103a, a few metres to the south, is dominated by a vermetid reef 23 m above sea level, which incorporates *Crassostrea* as well as the species present in site 103 b, *S. gaederopus* and abundant *G. glycymeris*. It shows that emergence here amounted to about 24 m in the last 34000 years, and its age, about 2000 years greater than that for 103b, is consistent with its position 3 m lower in the sequence.

At Cape Heraion itself the borings and marine deposits reported by Imperatori (1961) near the lighthouse can be traced into the embayment occupied by the ancient site of Perachora. Patches of reef material are to be found in numerous exposures between Cape Heraion and Vouliegmeni. The sandy beds west of the harbour consist predominantly of reefs incorporating *G. glycymeris* as well as *Pecten* and *Chlamys*. Deposits containing *Crassostrea* are found nearby, 13 m above sea level. It is reasonable to take this as a minimum value for the emergence that took place during the last 32000 years and is dated by the date for site 915.

Within the Vouliegmeni lagoon, mollusc borings which are probably intertidal in origin are found at heights of 1.5 m and 4 m above present sea level in a cliff east of the canal. When the Pleistocene marine terraces on the coasts of the peninsula were lifted, the lagoon was doubtless cut off from the sea. The present barrier, which is composed of soft serpentinized volcanics, is about 3.5 m high. The dated shells in the canal may correspond with the 1.5 m level within the lagoon, in which case an artificial connection to the sea by 7000 years ago has to be postulated. Alternatively, as *N. irus* is known to colonize older burrows, pre-existing intertidal borings may have been occupied by *N. irus* at some stage during the emergence that followed formation of the Pleistocene beaches and when the land neck was still submerged.

PHILOSOPHICAL TRANSACTIONS OF THE ROYAL SOCIETY A MATHEMATICAL, PHYSICAL & ENGINEERING SCIENCES

The edge of the Helladic site is below sea level, presumably because the early Helladic land level was slightly higher than the present. Movement along faults could explain submergence but such local motion would not account for the regional subsidence that took place in the 1981 earthquake, nor for the uplift of the Helladic site and of the jetty at Heraion in historical times. Whatever the precise chronology, or the amplitude of the various displacements, one may therefore conclude that during the last 32000 years the area has undergone uplift by about 25 m followed by subsidence and that the subsidence was interrupted by at least one phase of uplift.

Further east, at site 501, a series of shelly sands containing *Crassostrea* as well as *Pecten* and venerids is overlain by 30 cm of beach gravels containing *G. glycymeris*, *Crassostrea* and *C. vulgatum*. This in turn is overlain by 10 cm of gravelly beachrock and 1 m of shelly sands (figure 18, plate 2). The beachrock yields among other things abundant *C. vulgatum* and *Truncullariopsis trunculus*. The sands contain *S. gaederopus* at their base, and this species was employed to date that was taken to be a period of shallow water conditions for a level now 7.5 m above high water. Emergence by at least this amount dates from the last 36000 years.

(*c*) *Palaeontology*

The marked discrepancy between the ^{14}C dates obtained in the present study and the ages indicated by the palaeontological evidence adds weight to the view that many of the species used as stratigraphic markers in the Mediterranean Quaternary are of value only as facies indicators. Dufaure *et al.* (1975) and Schröder (1975) have pointed out that *Natica lactea* (*Polynices lacteus*), often equated with the Tyrrhenian, occurs in earlier deposits. *S. gaederopus* and *Conus mediterraneus*, reported from the Tyrrhenian of the Perachora peninsula by Mitzopoulos (1933, cited by Schröder 1970), are still common in the Mediterranean today. *Chlamys septemradiata*, used to identify Calabrian units (see, for example, Bousquet *et al.* 1976), is also still present and hence can at best serve as a post-Tertiary indicator (Dufaure *et al.* 1975).

The 'brackish-water' faunas that serve to identify the Apscheronian and Tchaudian levels of the Lower Pleistocene also present difficulties of interpretation. *Didacna fuchsi*, for instance, is viewed as a Tchaudian species, but this can only be on the grounds of its habitat preference as it is of Recent age in the Caspian (Moore 1969). The problem is compounded where redeposition is a possibility, as at the base of section Ie of Freyberg (1973) – our site 2 – where *D. fuchsi* is among the species that Sébrier (1977) suspects were derived from underlying strata. Again, when molluscs are too poorly preserved for determination to the species level it is perhaps safer to shelve any chronological attribution. The 500 m terrace in the classic 'staircase' of supposed marine levels between Kiaton and Souli has yielded the casts of *Cardium* sp., *Bittium* sp. and *Venus* sp. The absence of shell material and the fact that identification could not go beyond the genus level raise the possibility of redeposition: the beds need not be either Pleistocene or marine.

The 600–700 m level in this sequence appears to have produced no marine fossils at all, but this is not surprising in view of the predominance of fluviatile and slope deposits in the exposures along this transect. The highest unambiguously marine terrace that bears on the present account is the 200 m level at Kiaton, where Keraudren (1970–2) reported a 'banal' littoral fauna as well as a Tchaudian component (*D. fuchsi* and *Adelinella elegans*). Keraudren ascribed the terrace to the Milazzian (Mindel-Riss), after dismissing the Tchaudian elements as reworked, even though he was elsewhere willing to countenance uplift of the Tyrrhenian beaches south of Corinth to 210–220 m (rather than the 350 m of previous authors).

PHILOSOPHICAL TRANSACTIONS OF THE ROYAL SOCIETY A MATHEMATICAL, PHYSICAL & ENGINEERING SCIENCES

Table 1. Radiocarbon ages obtained for this study

lat. and long. (see figure 3)	height above high water/m	species	X.r.d[1]	^{14}C age (years B.P.)[2]	lab. no.	δ^{13}C (‰)[3] A	δ^{13}C (‰)[3] B	comments
38° 02′ 56″ N 22° 51′ 29″ E	23	*Glycymeris glycymeris*	A	33580^{+850}_{-760}	SRR-2241	1.6	1.7	
38° 02′ 56″N 22° 51′ 29″ E	20	*Arca noae*	A	31820^{+660}_{-630}	SRR-2245	1.2	1.0	
38° 02′ 30″ N 22° 51′ 14″ E	8	*Glycymeris glycymeris*	A	32440^{+670}_{-610}	SRR-2242	1.8	1.6	
38° 02′ 18″ N 22° 52′ 37″ E	1.7	*Notirus irus*	A	6890 ± 90	SRR-2244	−1.3	−1.0	7100 ± 1300 years B.P. (UCL-10) (Vita-Finzi 1983)
38° 02′ 01″ N 22° 53′ 10″ E	23.5	*Arca noae*	A	32060^{+740}_{-690}	SRR-2247	0.4	0.0	
38° 00′ 48″ N 22° 55′ 37″ E	7.5	*Spondylus gaederopus*	A +3% C	36180^{+1200}_{-1030}	SRR-2246	0.2	1.1	Mixed mineralogy is characteristic of Spondylidae (Taylor *et al.* 1969).
37° 56′ 55″ N 22° 58′ 00″ E	12	*Pinna fragilis*	A +9% C	38320^{+1590}_{-1340}	SRR-2240	1.7	1.4	Mixed mineralogy is characteristic of Pinnacea (Taylor *et al.* 1969).
37° 55′ 12″ N 23° 00′ 24″ E	0.5	*Crassostrea* sp.	C	35680^{+1450}_{-1210}	SRR-2339	−2.5	−1.7	
37° 56′ 24″ N 22° 57′ 02″ E	≈24	*Glycymeris glycymeris*	A	35680^{+1170}_{-1020}	SRR-2341	1.3	1.6	
37° 55′ 57″ N 22° 54′ 10″ E	25	*Cerastoderma glaucum*	A	31530^{+670}_{-610}	SRR-2243	1.3	1.3	Sébrier (1977) reports U-series age of 49000 ± 20000 on the terrace in question ('New Corinth').
37° 55′ 57″ N 22° 54′ 10″ E	26	*Cerastoderma glaucum*	A	30830^{+970}_{-860}	SRR-2342	1.1	1.3	
37° 55′ 53″ N 22° 52′ 52″ E	10.5	*Venus verrucosa*	A	30840^{+590}_{-560}	SRR-2248	−0.7	−1.0	
37° 54′ 43″ N 22° 53′ 52″ E	≈ 90	*Crassostrea* sp.	C	30670^{+570}_{-530}	SRR-2337	−3.5	−5.2	
37° 54′ 44″ N 22° 53′ 42″ E	≈ 90	*Crassostrea* sp.	C	31800^{+670}_{-620}	SRR-2340	−3.6	−2.8	
37° 54′ 40″ N 22° 56′ 18″ E	70	*Crassostrea* sp,	C	34870^{+990}_{-880}	SRR-2333	−2.4	−1.3	
37° 54′ 44″ N 22° 52′ 44″ E	≈ 25	*Mytilus galloprovincialis*	C +2% A	41770^{+2750}_{-2060}	SRR-2343	−2.0	−1.5	Some species of *Mytilus* have a mixed mineralogy (Milliman 1974; Taylor *et al.* 1969).

alculated by peak intensity method. A, aragonite with no detectable calcite. C, calcite with no detectable aragonite.
ormalized to $\delta^{13}C = 0‰$.
was determined on an aliquot from the bulk CO_2 prepared for dating and may thus reflect any fractionation induced in the laboratory; it is used normalization. B was determined on CO_2 from a separate subsample of shell by hydrolysis with H_3PO_4 at 25 °C (D. D. Harkness, personal nication) and is used here as a guide to sample quality
ge reported as > 40 420 by dating laboratory ($\delta^{14}C = -994.5 \pm 1.6‰$).

(*d*) *Discussion*

Table 1 summarizes the available information about radiocarbon ages and heights. It raises an issue that is familiar to Quaternary geologists, namely the extent to which ^{14}C ages of over 30000 years on shell are the products of contamination near the limits of the method rather than genuine ages. The precautions taken to exclude contaminated samples are evidently not foolproof. For example, peak-intensity analysis of the X-ray diffraction data has at best an

accuracy of 1% (Milliman 1974), and in any case the analysis, like microscopic inspection (figure 21, plate 2), is applied to small subsamples which may not be representative of the material dated. Should contamination by modern carbon amount to 1%, the real age of sample 103a could thus prove to be 50000–60000 years; contamination to varying degrees might have similar apparent ages for samples whose real ages differ widely. On the other hand, the agreement between ages for individual features is good (see for example 3c, 912/1, B2/101, B6/103, all on the Corinth/Old Corinth terrace), and at individual sites the older ages come from the lower stratum (103a and b; 2a and 3c). Moreover, the bulk and the subsample $\delta^{13}C$ results support the microscopic and X-ray diffraction (X.r.d.) evidence for lack of recrystallization in the aragonitic samples. The $\delta^{13}C$ values are lower among the calcitic specimens, which are in any case less readily screened (Vita-Finzi 1980), but even if these are shelved, aragonitic samples give very similar ages for features both on the Perachora peninsula (103, 915 and 502) and near Corinth (2, 3 and 912).

The close similarity in the ^{14}C ages of the terraces in the Perachora Peninsula and the Corinth area thus indicate that, as suggested by Herforth & Richter (1979) for Perachora, synchronous features have been displaced into a variety of elevations, presumably by faulting. The one locality where successive marine terraces are reported next to one another is the section exposed by the new Argos road, but the higher terrace turns out to be caprock material from the Pliocene land surface and not a fossil beach.

The palaeontological evidence from the eastern Gulf of Corinth neither supports nor contradicts these conclusions. The faunal assemblages are strongly influenced by local environmental conditions and cannot be used as time markers. But the terrace faunas may prove of value in identifying depositional environments and in so doing remove the constraints imposed by the assumption that the molluscs correspond to certain limited altitudes. Some of the brackish-water assemblages mentioned earlier could thus represent lakes which formed above sea level, whereupon their current elevation becomes irrelevant. Note that the older Neogene, probably over 1500 m thick in the northern Peloponnese, is characterized by marls indicative of brackish to lacustrine conditions; and the younger Neogene, up to 600 m thick and in places 1600 m above sea level, consists predominantly of fluvio-lacustrine deposits (Dercourt 1964; Kelletat *et al.* 1976).

4. Evolution of the eastern Gulf of Corinth

For our discussion of regional evolution we adopt a model based on the simplified section shown in figure 22. It is similar to the scheme proposed by Jackson *et al.* (1982) but the major faults are represented as fault zones rather than individual faults. Without this modification it is impossible to interpret some of the uplift data.

Information on vertical motion comes from two main areas designated α and β. The information for α lies between faults I and II and the information for β from the hanging wall of fault II. Zone α_1 is influenced by minor motion at the edge of system I (e.g. deformation of the 'New Corinth' terrace) and α_2 is disturbed by some of the faulting and downwarping on the Perachora peninsula. Zone β is affected by presumed offshore antithetic faulting.

The modelling in Jackson *et al.* (1982) (see figure 1*a*) indicates that movement on normal faults is distributed as 90% dropping of the hanging wall and 10% uplift of the footwall. These are reduced by about a factor of two at a distance of one fault depth (*ca.* 15 km) from the causal

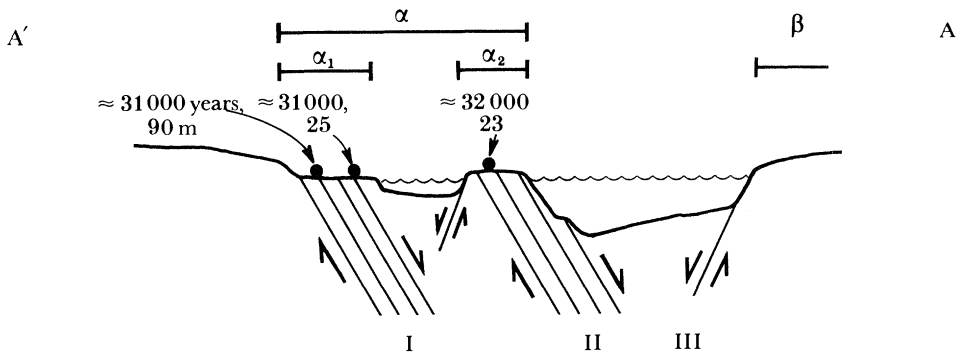

FIGURE 22. Schematic section along line AA′ (figure 7) showing the relationship between the main fault systems (I, II and III) and the zones (α and β) for which there is evidence for vertical displacement.

fault. From this we can see movement on fault I drops zone α by between 90% and 45% of the throw on that fault.

Fault II has the effect on β of dropping it by perhaps as much as 45% of the throw, allowing for antithetic faulting by 20%. This estimate is corroborated by the changes of level in the recent earthquake, where point Z on figure 3 dropped by 1.0 m and the coast near Porto Germano by 0.3 m. Motion of fault II lifts region α, zone α_1, by 10% of the fault throw and α_2 by 5%. Some points in α_2, however, are within the zone of faulting and downwarping of the system II and may go down or up depending on which part of the system is activated. Apparently the recent earthquake caused downwarping and subsidence of the peninsula. Motion on the more northerly faults will cause uplift, as observed in the recent earthquake at Y (figure 3) further along the coast where the main fault is offshore.

We can now consider the significance of our historical, archaeological and radiometric data in terms of motion on our simplified fault systems. Any attempt to derive absolute uplift from the various items of evidence would consider sea-level fluctuations and thus risk becoming enmeshed in inconclusive controversy. For this reason the ensuing discussion speaks of uplift or subsidence either by comparing contemporaneous features or by assuming, after Flint (1971) and many others, that, as sea level was lower than it is now during the period at issue, any of our dated shorelines now above the sea have undergone net uplift.

The salient points may be recapitulated in terms of their location in figure 12 as follows. Although the Perachora peninsula in α_2 subsided in 1981, exposed coastal notches indicate recent uplift. This is supported by the uplifted *diolkos* in α_1, and the uplifted jetty in α_2. In a similar historical period other regions have subsided both on the northern side of the Gulf and near *Cenchreae* (α_1). Before this period, however, the Perachora region α_2 subsided, although it had been higher than at present in Helladic times (5000 years ago). During the period extending to about 32000 years ago α_1 and α_2 have been uplifted and now stand in places over 20 m above the present sea level. The difference in height between various sites near Corinth we attribute to local faulting and take the highest (site 2) to represent maximum uplift.

Two features of the history of faulting emerge from the above.

(1) Up and down motions of zone α have occurred both in recent and in historical times. This requires activity on both fault system I and fault system II, an inference supported by the fact that the 1981 event occurred on II and that historical seismicity is known for system I (figure 23).

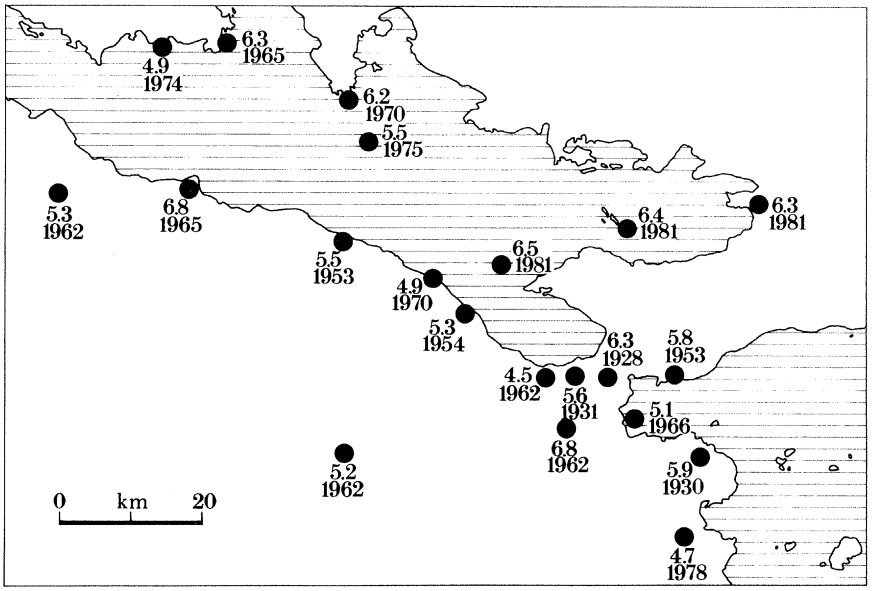

FIGURE 23. Epicentral locations of earthquakes in the Gulf of Corinth since 1902. The locations are taken from Papazachos *et al.* (1982) and are based on damage distribution as well as instrumental location. Date and magnitude are given beside each location.

(2) We observe total uplift around Corinth approaching 200 m. The maximum throw on fault system II is 1300 m without allowing for displacement concealed by sediment, which might possibly be more than 700 m thick. All of the observed motion on II plus motion we cannot see is required to account for the observed uplift. Motion on system I must have become very small before system II started moving, otherwise the large observed uplift would have been prevented by downdropping.

Assuming that the mechanism of uplift that we postulate is correct, the two statements are only compatible if the motion of fault system I that we observe in seismic activity and historical motion represents reactivation after a long period of quiescence. The present rate of motion on fault system I of 2 m in 2000 years is sufficient to annul the uplift effect of 20 m of motion on system II in the same period. If such motion on system I had continued for a long period, then high raised beaches could not have been created. We therefore assume that fault I scarcely moved for a long period before historical times. Broadly, the evolution is similar to that proposed by Jackson *et al.* (1982) but it is clear that the faults south of Corinth have been reactivated and now take part in the active deformation.

Our arguments assume that no Quaternary raised beaches are to be found above 200 m, a view based on our inspection of only some of the sites described in the literature; and our discussion of the uplift-to-subsidence ratio is based on the belief that normal faulting alone cannot create uplifts of more than 10% of total fault motion. The plausibility of such a ratio is based on arguments that rely on elastic deformation modelling described for normal faulting in Jackson *et al.* (1982) and for thrust faulting by King & Vita-Finzi (1981) and King & Brewer (1983). Isostatic considerations are discussed by Jackson & McKenzie (1983), but only on the basis of faulting which completely cuts the crust. Neither the elastic-based models nor the isostatic models can, at present, accommodate possible creep deformation or isostatic compensation at the level of the lower crust; nor do they consider complex fault geometries.

Similar problems in relation to the earthquake cycle are considered by Rundle & Thatcher (1980).

An allowance for these effects might permit normal faulting to create greater uplift. But, in the absence of convincing evidence that uplift greater than 200 m has occurred, a description based on simple extensional faulting accounts for the observed features of the eastern Gulf of Corinth without the need for compressional episodes. Deformation models more complex than the simple ones that we adopt are not at present required. The ^{14}C ages imply 220 m of motion on fault system II during the last 30000 years. At a constant rate this would give an earthquake repeat time for events with 2 m of slip (magnitude *ca.* 6.5, the same size as the 1981 events) of about 300 years per 20 km of fault.

5. Conclusions

We have examined the structure of the eastern Gulf of Corinth using information gained from studies of the 1981 earthquakes as a key to the relationship between deep and superficial structures. Historical, archaeological and ^{14}C dating of shorelines provides information on which to base an outline for the evolution of the area during the last 40000 years. For earthquakes such as those that occurred in 1981 a repeat time of about 300 years is found; the same rate of motion would form the Alkyonidhes Gulf in 180000 years. In the course of our study we have reached or reaffirmed the following conclusions of general application.

(1) Surface faults which produce major escarpments for long relatively linear segments are capable of producing repeated earthquakes with magnitudes greater than 6.0.

(2) Bends in the main trends of faulting are associated with multiple, shorter faults at depth. These are associated with smaller earthquakes, and the effect of cumulative motion is to produce surface folding.

(3) The surface folding may be associated with secondary faulting, which can form clear surface features but is not a direct manifestation of the major faulting at depth.

(4) Historical, archaeological and ^{14}C dating of displaced shorelines provides a powerful method of determining the evolution of an active region provided that sufficient information about fault geometry is available.

(5) The dating of shell material using ^{14}C can be effective for ages up to 40000 years if samples are prepared carefully. This method is preferable to the palaeontological dating of marine terraces, which in the Mediterranean can be misleading because the species are controlled primarily by environment.

(6) Terrace features assumed to be distinguishable in age by virtue of their height above sea level may prove to be contemporaneous; differences in elevation due to tectonic motion can be used for testing and calibrating structural models.

Many of the techniques adopted in this study can be applied in other parts of the world but it is clear that an extensive historical and archaeological record linked to a long coastline makes the Aegean of unique value to studies of recent tectonics.

We are indebted to the N.E.R.C. for the ^{14}C dates and for a grant to cover the cost of fieldwork, to Dr D. D. Harkness for supervising the age determinations, to M. T. Beleza and L. Vita-Finzi for assistance in the field and to Dr D. H. Matthews, Dr G. W. Richards and Professor R. Tomlinson for assistance and discussions. This is Cambridge Department of Earth Sciences contribution number 583.

PHILOSOPHICAL TRANSACTIONS OF THE ROYAL SOCIETY A MATHEMATICAL, PHYSICAL & ENGINEERING SCIENCES

References

Aki, K. 1979 Characterization of barriers on an earthquake fault. *J. geophys. Res.* **84**, 6140–6148.

Bally, A. W. 1982 Musings over sedimentary basin evolution. *Phil. Trans. R. Soc. Lond.* A **305**, 325–338.

Benson, E. F. 1895 Aegosthena. *J. Hellenic Stud.* **15**, 314–324.

Bousquet, B., Dufaure, J.-J., Keraudren, B., Péchoux, P.-Y., Philip, H. & Sauvage, J. 1976 Les corrélations stratigraphiques entre les faciès marins lacustres et continentaux du Pléistocène de Grèce. *Bull. Soc. géol. Fr.* **18**, 413–418.

Brooks, M. & Ferentinos, G. 1984 Tectonics and sedimentation in the Gulf of Corinth and the Zakynthos and Kefallinia Channels, western Greece. *Tectonophysics* **101**, 25–54.

Depéret, Ch. 1913 Observations sur l'histoire géologique pliocène et quaternaire du golfe et de l'isthme de Corinthe. *C. r. hebd. Séanc. Acad. Sci., Paris* **156**, 426–431, 659–663, 1048–1052.

Dercourt, J. 1964 Contribution à l'étude géologique d'un secteur du Péloponnèse septentrional. *Ann. Géol. Pays Hell.* **XV**, 1–418.

Dufaure, J.-J., Kadjar, M-H., Keraudren, B., Mercier, J.-L., Sauvage, J. & Sébrier, M. 1975 Les déformations plio-pleistocènes autour du golfe de Corinthe. *C. R. Somm. Soc. géol. Fr.*, pp. 18–20.

Dziewonski, A. M. & Woodhouse, J. 1983 An experiment in systematic study of global seismicity: centroid moment tensor solutions for 201 moderate and large earthquakes of 1981. *J. geophys. Res.* **88**, 3247–3271.

Fink, R. & Schröder, B. 1971 Anzeichen eines holozänen Meereshochstandes an der Landerige von Korinth. *Neues Jb. Paläont. Mh.* **5**, 265–270.

Flemming, N. C. 1978 Holocene eustatic changes and coastal tectonics in the northeast Mediterranean: implications for models of crustal consumption. *Phil. Trans. R. Soc. Lond.* A **289**, 405–458.

Flint, R. F. 1971 *Glacial and quaternary geology*. New York: Wiley.

Fossey, J. M. 1969 The prehistoric settlement by Lake Vouliagmeni, Perachora. *Ann. Br. Sch. Athens* **64**, 53–69.

Freyberg, B. von 1973 Geologie des Isthmus von Korinth. *Erlanger geol. Abh.* **95**, 1–183.

Heezen, B. C., Ewing, M. & Johnson, G. L. 1966 The Gulf of Corinth floor. *Deep-Sea Res.* **13**, 381–411.

Herforth, A. & Richter, D. K. 1979 Eine pleistozäne tektonische Treppe mit marinen Terrassensedimenten auf der Perachorahalbinsel bei Korinth (Griechenland). *Neues Jb. Geol. Paläont, Abh.* **159**, 1–13.

Imperatori, L. 1961 Livelli quaternari nel Golfo di Corinto e nel Sud del Peloponneso. *Quaternaria* **5**, 131–133.

Ivanovich, M., Vita-Finzi, D. & Hennig, G. J. 1973 Uranium-series dating of molluscs from uplifted Holocene beaches in the Persian Gulf. *Nature, Lond.* **302**, 408–410.

Jackson, J. A., Gagnepain, J., Houseman, G., King, G. C. P., Papadimitriou, P., Soufleris, C. & Virieux, J. 1982 Seismicity, normal faulting, and the geomorphological development of the Gulf of Corinth (Greece): the Corinth earthquakes of February and March 1981. *Earth planet. Sci. Lett.* **57**, 377–397.

Jackson, J. A. & McKenzie, D. P. 1983 The geometrical evolution of normal fault systems. *J. struct. Geol.* **5**, 471–482.

Kelletat, D., Kowakzyk, G., Schröder, B. & Winter, K.-P. 1976 A synoptic view on the neotectonic development of the Peloponnesian coastal regions. *Z. Dt. geol. Ges.* **127**, 447–465.

Keraudren, B. 1970–2 Les formations quaternaires marines de la Grèce. *Bull. Mus. anthrop. préhist. Monaco* **16**, 5–153, **17**, 87–169, **18**, 245–279.

King, G. 1985 The accommodation of finite strain in the upper lithosphere of the earth by self-similar fault systems: the geometrical origin of b-value. *Pure appl. Geophys.* **121**, 761–815.

King, G. & Stein, R. 1984 Surface folding, river terrace deformation rate and earthquake repeat time in a reverse faulting environment: the Coalinga, California, earthquake of May 1983. In *The 1983 Coalinga, Calif. Div. Mines Geol. Spec. Publ.* **66** (In the press.)

King, G. C. P. & Brewer, J. 1983 Fault related folding near the Wind River thrust, Wyoming, USA. *Nature, Lond.* **306**, 147–150.

King, G. C. P. & Vita-Finzi, C. 1981 Active folding in the Algerian earthquake of 10 October 1980. *Nature, Lond.* **292**, 22–26.

King, G. C. P., Ouyang, Z. X., Papadimitriou, P., Deschamps, A., Gagnepain, J., Houseman, G., Jackson, J. A., Soufleris, C. & Virieux, J. 1985 The evolution of the Gulf of Corinth (Greece): an aftershock study of the 1981 earthquakes. *Geophys. Jl R. astr. Soc.* **80**, 677–693.

King, G. C. P. & Yielding, G. 1984 The evolution of a thrust fault system: processes of rupture initiation, propagation and termination in the 1980 El Asnam (Algeria) earthquake. *Geophys. Jl R. astr. Soc.* **77**, 915–933.

Le Pichon, X. & Angelier, J. 1979 The Hellenic trench system: a key to neotectonic evolution of the eastern Mediterranean area. *Tectonophysics* **60**, 1–42.

McKenzie, D. P. 1978 Active tectonics of the Alpine–Himalayan belt: the Aegean Sea and surrounding regions. *Geophys. Jl R. astr. Soc.* **55**, 217–254.

Mansinha, L. & Smylie, D. E. 1971 The displacement fields of inclined faults. *Bull. seismol. Soc. Am.* **61**, 1433–1440.

Mariolakos, I., Papanikolaou, D., Symeonidis, N., Lekkas, S., Zarotsieris, Z. & Sideris, Ch. 1982 The deformation of the area around the eastern Korinthian Gulf, affected by the earthquakes of February–March 1981. *Proc. Int. Symp. Hellenic Arc & Trench*, Athens, vol. I, pp. 400–419.

PHILOSOPHICAL TRANSACTIONS OF THE ROYAL SOCIETY A MATHEMATICAL, PHYSICAL & ENGINEERING SCIENCES

Milliman, J. D. 1974 *Marine carbonates*. New York: Springer-Verlag.
Moore, R. C. (ed.) 1969 *Treatise on invertebrate paleontology: N2*. Boulder: Univ. Kansas Press and Geol. Soc. Am.
Papahatzis, N. 1981 *Ancient Corinth*. Athens: Ekdotike Athenon SA.
Papazachos, B. C., Comninakis, P. E., Hatzidimitriou, P. M., Kiriakidis, E. G., Kyratzi, A. A., Panagiotopoulos, D. G., Papadimitriou, E. E., Papaioannou, Ch. A., Pavlides, S. B. & Tzanis, E. P. 1982 *Atlas of isoseismal maps for earthquakes in Greece 1902–1981. Geophys. Lab. Univ. Thessaloniki, Publ.* **4**.
Payne, H. 1940 *Perachora*, vol. I. Oxford: Clarendon Press.
Richards, G. W. 1982 Intertidal molluscs as sea-level indicators: a comparative study of modern and fossil Mediterranean assemblages. Ph.D. thesis, London University.
Richter, D. K., Herforth, A. & Ott, E. 1979 Pleistozäne, brackish Blaugrünalgenriffe mit *Rivularia haematites* auf der Perachorahalbinsel bei Korinth (Griechenland). *Neues Jb. Geol. Paläont. Abh.* **159**, 14–40.
Rundle, J. B. & Thatcher, W. 1980 Speculations on the nature of the southern California uplift. *Bull. seismol. Soc. Am.* **70**, 1869–1886.
Schröder, B. 1970 Über mittel- und jung-pleistozänes Meeres-Hochstände der Landenge von Korinth. *N. Jb. Geol. Paläont. Mh.* **1**, 27–33.
Schröder, B. 1975 Bemerkungen zu marinen Terrassen des Quartärs im NE-Peloponnes/Griechenland. *Neues Jb. Geol. Paläont. Abh.* **149**, 148–61.
Schwandner, E.-L. 1977 Die Böotische Hafenstadt Siphai. *Arch. Anzeiger*, pp. 513–551.
Scranton, R. L. & Ramage, E. S. 1967 Investigations at Corinthian Kenchreai. *Hisperia* **36**, 124–186.
Sébrier, M. 1977 Tectonique récente d'une transversale à l'Arc Egéen: Le Golfe de Corinthe et ses régions périphériques. Thesis, Univ. Paris XI.
Stearns, C. E. & Thurber, D. L. 1967 Th^{230}/U^{234} dates of late Pleistocene marine fossils from the Mediterranean and Moroccan littorals. *Prog. Oceanogr.* **4**, 293–305.
Taylor, J. D., Kennedy, W. J. & Hall, A. 1969 The shell structure and mineralogy of the Bivalvia. Introduction. Nuculacea–Trigonacea. *Bull. Br. Mus. nat. Hist.* (*Zool.*) Suppl. 3.
Vita-Finzi, C. 1978 *Archaeological sites in their setting*. London: Thames & Hudson.
Vita-Finzi, C. 1980 ^{14}C dating of recent crustal movements in the Persian Gulf and the Iranian Makran. *Radiocarbon* **22**, 763–773.
Vita-Finzi, C. 1983 First-order ^{14}C dating of Holocene molluscs. *Earth planet. Sci. Lett.* **65**, 389–392.
West, R. G. 1968 *Pleistocene geology and biology*. London: Longmans.

PHILOSOPHICAL TRANSACTIONS OF THE ROYAL SOCIETY A MATHEMATICAL, PHYSICAL & ENGINEERING SCIENCES

FIGURE 9. View east in the direction of the arrow in figure 4. The sketch indicates the main structural features, including a deformed raised beach. Level A appears to correspond to the terrace at site 103 (table 1, figure 19 (plate 2)).

PHILOSOPHICAL TRANSACTIONS OF THE ROYAL SOCIETY A MATHEMATICAL, PHYSICAL & ENGINEERING SCIENCES

GURE 11. View north in the direction of the arrow in figure 8 and figure 10*d*. Acrocorinth (right) was an outcrop of limestone protruding through the marls and caprock of the pre-faulting erosion surface. The marls are now subject to badland erosion resulting from backtilting and a drop of river level due to faulting between Acrocorinth and the sea. The marls and caprock are folded, requiring similar deformation of the limestone of Acrocorinth.

FIGURE 12. A view north along the river valley between sections *b* and *c* of figure 8. Note the caprock (upper left), which is conformable with the uneroded land surface and the marl beneath. It is this conformable relationship which makes it possible to use topographic sections for determining the deformation of the underlying strata resulting from buried faults.

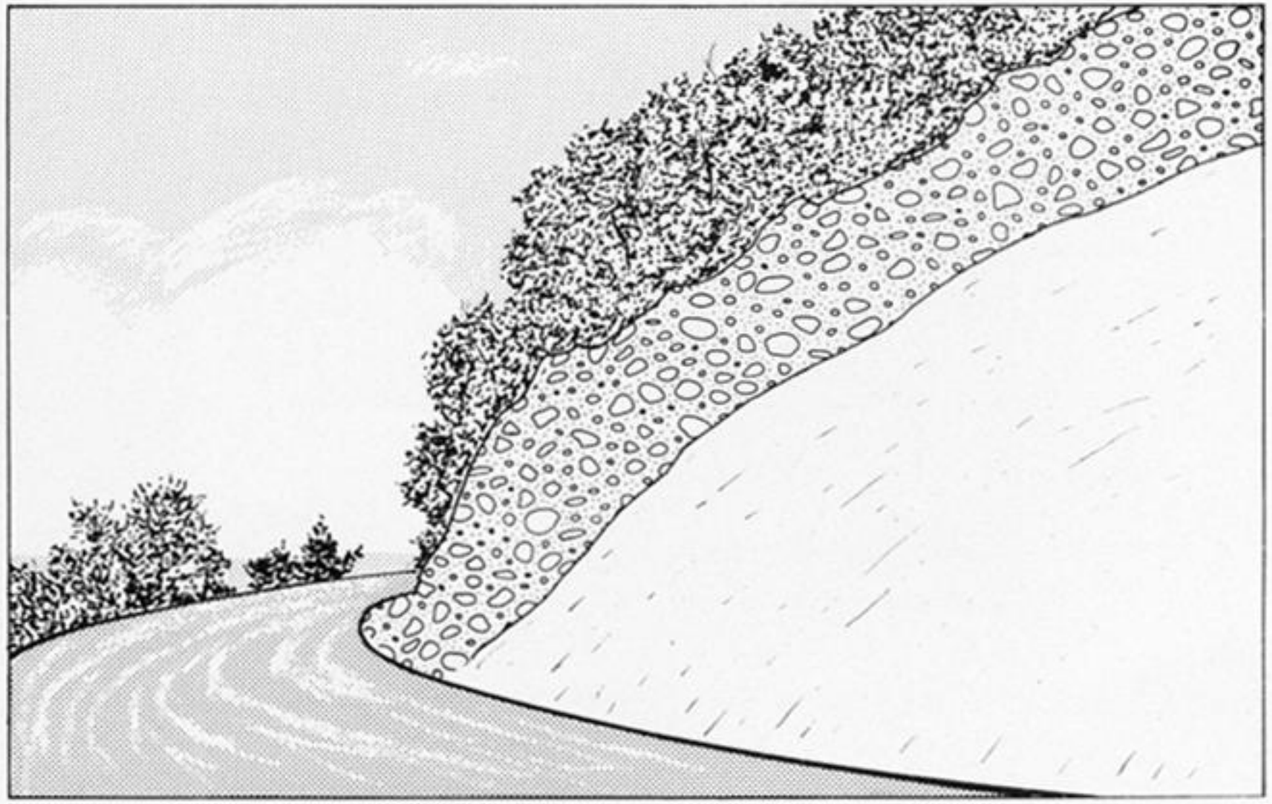

FIGURE 15. Folding of the caprock over a buried fault on the Kiaton road (see A in figure 14). The caprock is composed of sands and gravels of continental origin. In some places it is clearly fluviatile. In general the composition is coarser and the caprock thicker (up to 3 m) near the hills, and it becomes finer and thinner near the coast where it is also mixed with beach deposits. The caprock results from the transgression of debris from the adjacent mountains over the marls as the sea or lake in which they were deposited retreated. In some places (including this location) marls are interbedded with the caprock near the surface indicating that the retreat was not monotonic. Caprock covers the marls and is conformable with the land surface except where it has been removed by badland erosion or where limestone outcrops rise above the old lake surface (see figure 11).

PHILOSOPHICAL TRANSACTIONS OF THE ROYAL SOCIETY A MATHEMATICAL, PHYSICAL & ENGINEERING SCIENCES

GURE 16. Beachrock overlying the ramp used to drag boats across the Isthmus of Corinth in antiquity. The upper surface of the beach rock is about 0.5 m above present high water. The beachrock is certainly younger and possibly much younger than the ramp.

FIGURE 17. A view of site 103b from the sea. The upper beds are marine in origin and overlie the marls unconformably. An unconformable contact is usual between these deposits, whereas the contact between caprock and marl is apparently always conformable.

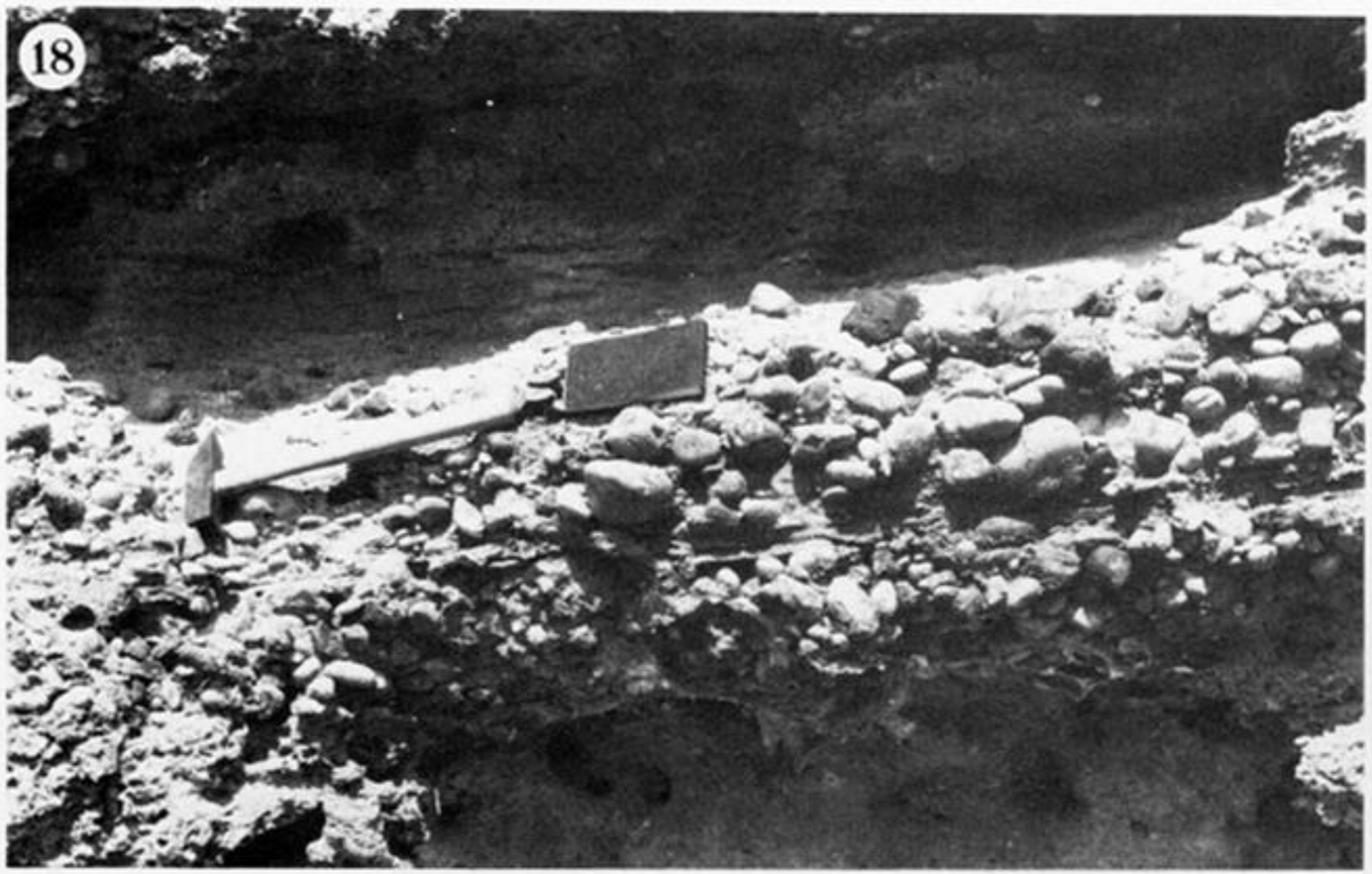

IGURE 18. Pebbles of the beach deposit at site 501. Identification of features such as this containing datable material enables the former waterline to be established to within 1 m.

GURE 19. Escarpment near site 2 (figure 3, table 1). Note the angular unconformity between the Pleistocene marine deposits and the underlying marl.

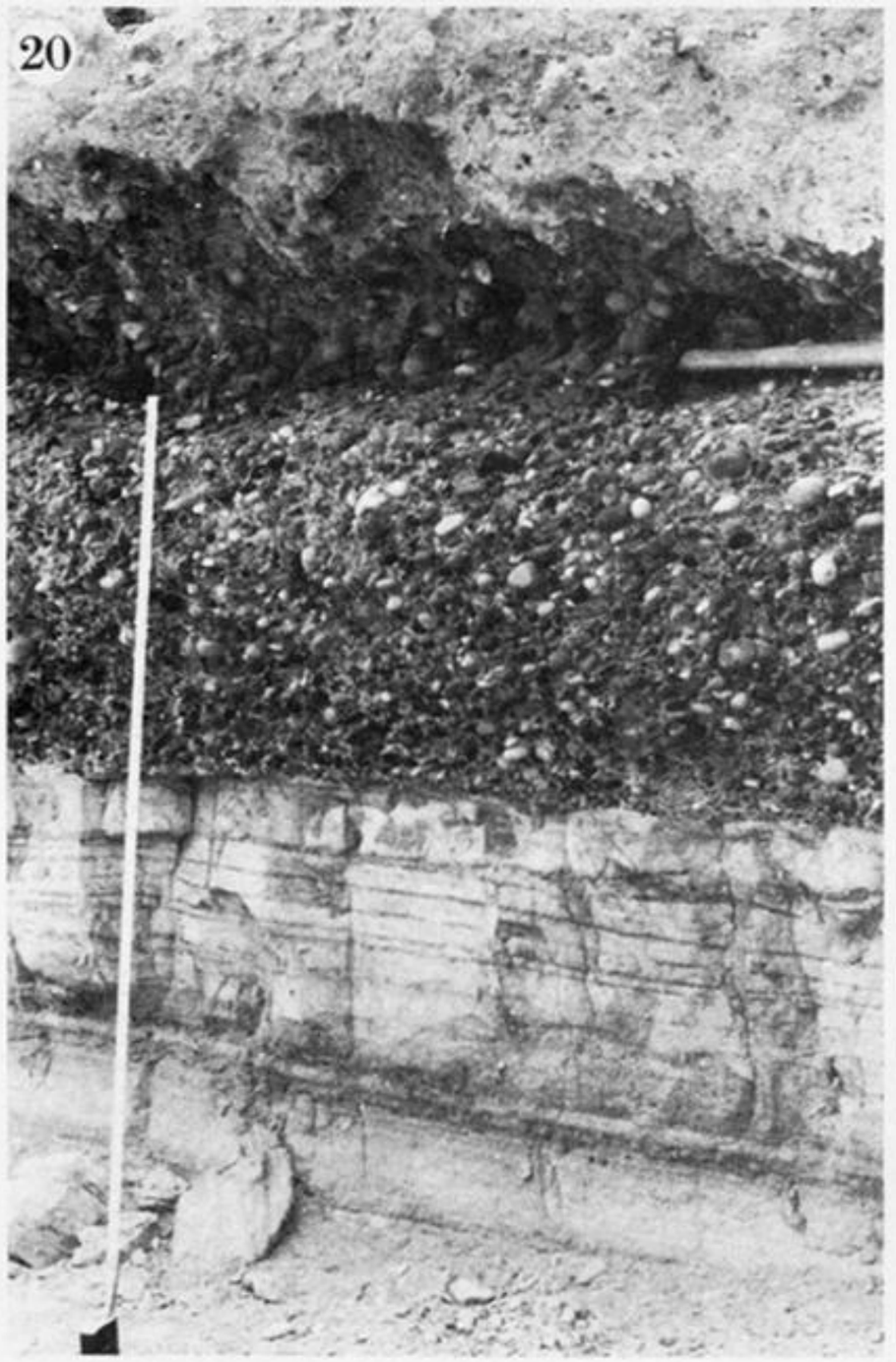

GURE 20. Caprock gravels conformably overlying marls and unconformably covered by beach gravels at site 2. The hammer indicates the unconformity.

PHILOSOPHICAL TRANSACTIONS OF THE ROYAL SOCIETY A MATHEMATICAL, PHYSICAL & ENGINEERING SCIENCES

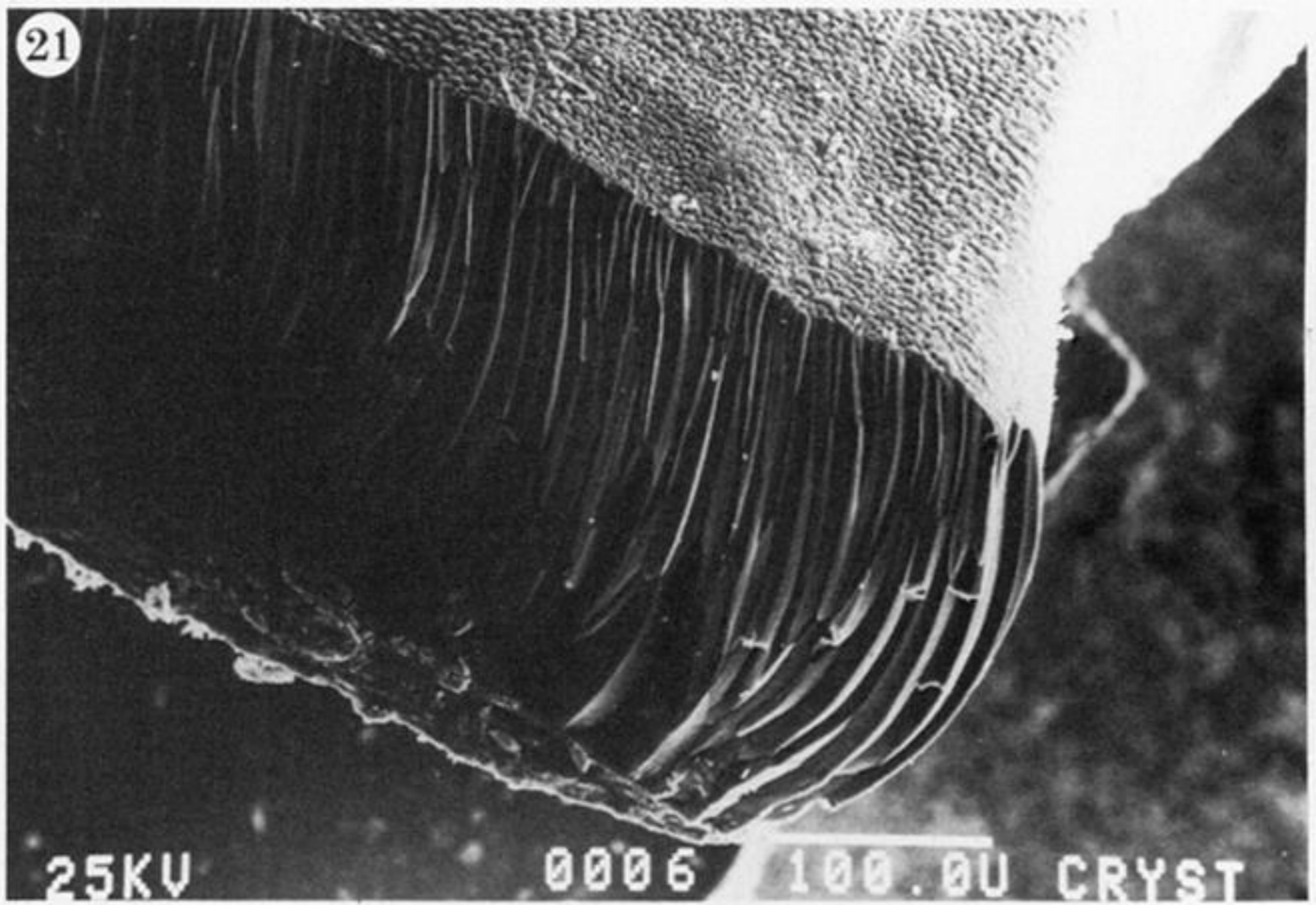

GURE 21. Scanning electronmicrograph of *Pinna fragilis* from site 302 showing calcitic prisms of outer shell layer. Note that all contamination is on the surface (lower left) and was therefore removed before dating. Scale bar represents 100 μm.